공학박사학위논문

스테인리스강 표면 젖음성에 대한 에이징 및 열처리 영향

Influence of Aging and Heat Treating on the Wettability of Stainless Steel Surface

2018 년 2 월

서울대학교 대학원

기계항공공학부

김 두 곤

스테인리스강 표면 젖음성에 대한 에이징 및 열처리 영향

Influence of Aging and Heat Treating on the Wettability of Stainless Steel Surface

지도교수 주 종 남

이 논문을 공학박사 학위논문으로 제출함

2017 년 10 월

서울대학교 대학원

기계항공공학부

김 두 곤

김두곤의 공학박사 학위논문을 인준함

2017 년 12 월

위 원 장 : 이 정 훈

부위원장 : 주 종 남

위 원 : 김 호 영

위 원 : 차 석 원

위 원 : 김 보 한

Abstract

Doogon Kim
School of Mechanical and Aerospace Engineering
The Graduate School
Seoul National University

Wettability control of engineering metals such as steel, copper, aluminum and their alloys is one of the future-promising technologies to enhance functionality of the materials used in various fields such as automobile, building, ocean plant, military, aerospace, *etc*. While significant amount of research output has been reported in laboratory scale, commercialization of the technology is still stagnant due to several difficulties. One representative example is aging effect on the wettability of engineering metals, which refers to time-dependent wettability transition from hydrophilic to hydrophobic state. This makes it difficult to achieve superhydrophobic and superhydrophilic metal surfaces.

In this dissertation, influence of aging and heat treating on the wettability of stainless steel surface is studied. Aging effect is investigated on a flat AISI

stainless steel 304 surface to understand the intrinsic wettability. The effect of oxygen is explained as a main cause for aging effect. Heat treating effect is investigated and revealed as a powerful process to tune the intrinsic wettability of stainless steel surface. Finally, wettability control without chemical coating is demonstrated for superhydrophobic and superhydrophilic stainless surfaces considering the effects of aging and heat treating.

Keywords: metal, stainless steel, surface, wettability, heat treating

Student number: 2014-30336

Contents

List of Figures

List of Tables

1. Introduction

1.1 Research background

Wettability, which refers to the wetting characteristic of a solid surface against a liquid, is one of key properties determining the functionality of a material. Examples can be found easily in nature, where marvelous wettability of biological surfaces plays a vital role in surviving ability of plants, insects and animals in nature.[1-2] A representative example is lotus leaves, inhabiting a muddy swamp. The surface of lotus leaves is famous for its water-repellency and self-cleaning properties, which help maintain the surface clean against mud, facilitating photosynthesis.[3] Another examples is fly eyes, whose anti-condensation property guarantee a clear vision in spite of variable weather and temperature.[4] These examples tell us that special wettability of a material surface enhances the functionality of a material even in a harsh environment.[5]

Wonderful examples in nature have been inspiring researchers in various fields in that special wettability can improve the potential of materials for diverse applications. Based on the fact that the structural geometry in submillimeter scale

as well as surface free energy of a material determines wettability,[6] researchers have been realizing artificial surfaces with special wettability, *i.e.*, fully-wetting or non-wetting to diverse liquids from water to organic solvents. Also, a variety of applications of artificial surfaces with special wettability have been extensively reported such as liquid separation, self-cleaning, anti-biofouling, anti-icing, drag reduction, anti-corrosion, *etc*., which suggests a future-promising effect of related technologies for wettability control of a material.[1]

Recently, wettability control of engineering metals such as steel, copper, aluminum and their alloys draws a significant attraction of researchers and engineers.[7] Because engineering metals have already been used in numerous industrial fields such as machinery, automotive, aerospace, building, maritime, military as a crucial material, wettability control technology for engineering metals is expected to yield a significant commercial impact as well as a large amount of added value to the today's applications by broadening applications to a more harsh operating environment and enhancing functionality. Behind this anticipation, the advance of fabrication technology strongly supports the feasibility. The resolution of today's micromachining technology for engineering metals reaches submillimeter scale where wettability is mainly governed combined with surface free energy of a material.[8] Not only does mechanical cutting process accomplish microscale work with ease, several non-contact machining methods such as laser-

beam machining, electrochemical machining, electrical discharge machining, *etc*., also handles engineering metals efficiently in submillimeter scale.[8-13]

An extensive effort has been put to develop various fabrication methods for wettability control of engineering metals based on micromachining processes for surface structuring. Surface structuring in a submillimeter scale is achieved by several methods such as etching, laser-beam machining, electrical discharge machining, sand-blasting, electrodeposition, etc.[7] It renders the surface of engineering metals have micro/nanoscale roughness, which is necessary to enhance the intrinsic wettability originated from surface free energy of a material.

There are two distinguishable ways to finalize a designed wettability on the surface of engineering metals: 1) adding a post-process of chemical treatment on top of the structured surface 2) realizing a designed wettability on a bare surface without chemical treatment. After the machining process for surface structuring, chemical treatment is usually applied on top of the structured surface to control the surface free energy in a suitable way for a designed wettability; in case of fabricating non-wetting surfaces, low-surface-energy chemicals are applied, such as fluorination.[14] Chemical treatment is instantly effective to realize a designed wettability in a laboratory scale, however, chemical treatments is limited to industrial applications requiring high robustness due to harsh operating conditions. [15-16] Alternatively, fabrication processes without chemical treatments have been

reported so far to overcome the problems as mentioned above.[17-23] This approach solely depends on surface structuring in submillimeter scale and utilizes the intrinsic wettability of mother materials, which gives more robust and suitable methods for industrial use because of its monolithic characteristics.

While wettability control without chemical treatment is expected to be a powerful approach for industrial use, there still remain a critical problem which has not been fully elucidated yet: aging effect on the wettability of engineering metals after surface structuring.[19, 21, 24-32] Aging effect refers to the wettability transition of surface from wetting state to hydrophobic state. After surface structuring, the surface is in wetting state. As time passes, the surface gradually changes wettability into hydrophobic state. Because of its time-dependent characteristics, aging effect makes it difficult to achieve well-controlled and homogeneous wettability.

Aging effect results in mainly two technical limitations of wettability control for engineering metals: 1) time-consuming process for superhydrophobic surfaces 2) difficulty in achieving superhydrophilic surfaces. Figure 1.1 shows challenges caused by aging effect. In case of making superhydrophobic surfaces without chemical treatment, it needs more than several days to eventually realize a designed wettability. In order to shorten the time required to realize super-hydrophobic state, heat treating was introduced as an effective way to accelerate

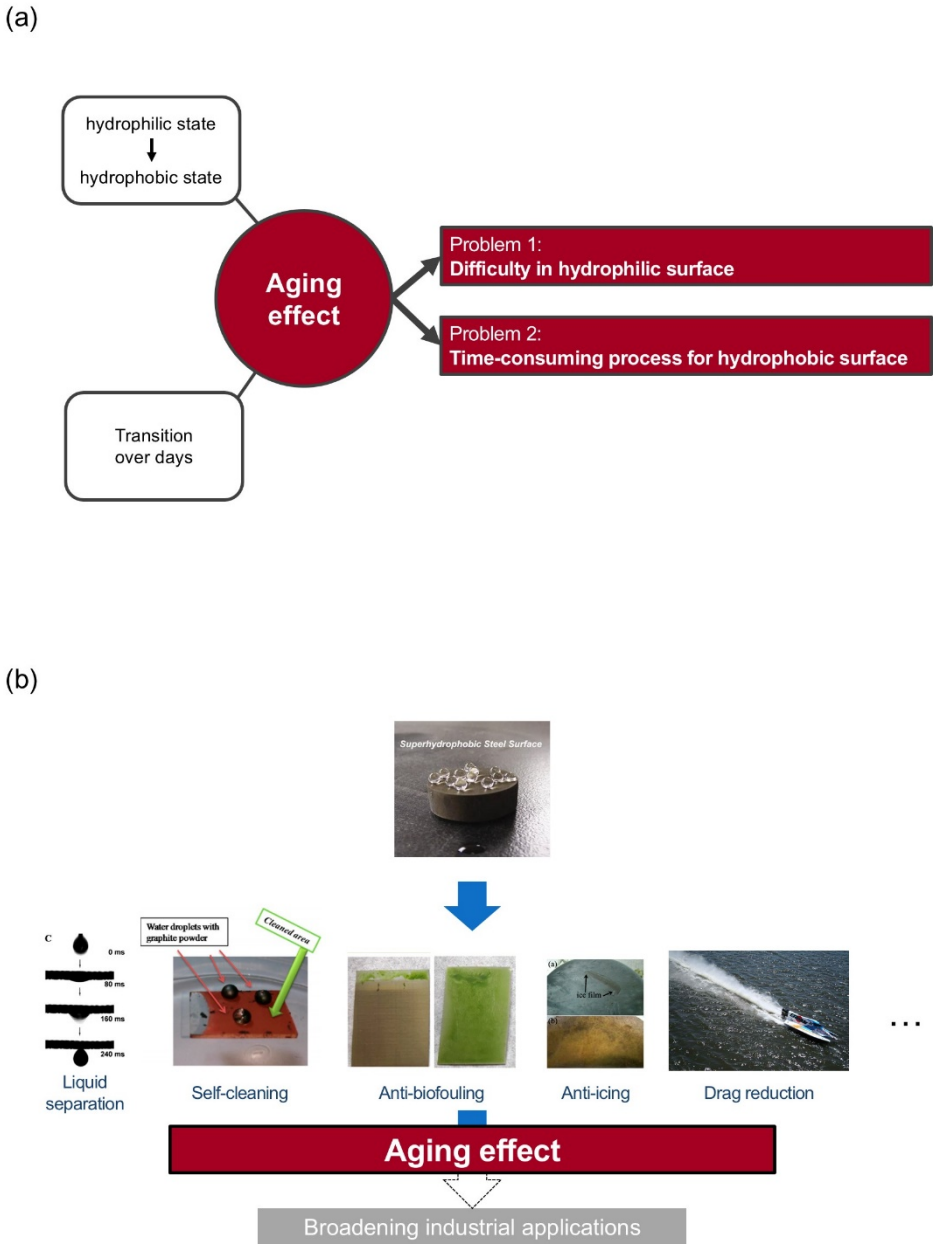

Figure 1.1 Schematic illustration of (a) difficulties resulted from aging effect on the wettability of engineering metals (b) challenges in the industry

the aging.[19, 32] But it was partially limited in that only a certain point of temperature was suggested to be effective without investigating the change of intrinsic wettability of material of interest. In case of making superhydrophilic surfaces without chemical treatment, initial superhydrophilic state is lost after several days from the time of surface structuring.

Commercial application of wettability control technology for engineering metals is delayed due to the problems mentioned above up to today, in spite of increasing amount of academic outputs and industrial interest. As presented in Figure 1.2, the number of reported research papers about “superhydrophobic” and “superhydrophilic” surfaces continuously increasing starting from 2000 to 2016. Today, however, it is still difficult to find examples of wettability control technology in mass-production scale. Therefore, it is timely to investigate the aging effect and find way of controlling it in consideration with intrinsic wettability of materials, which eventually enabling evidently feasible wettability control technology without chemical treatment for scalable, robust, and industry-friendly applications.

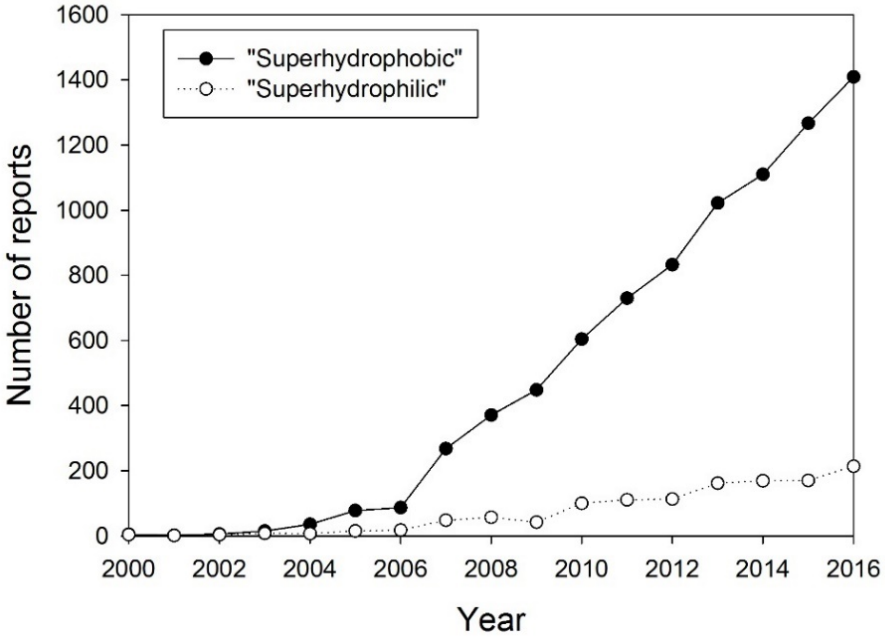

Figure 1.2 The number of reported research papers about “superhydrophobic” and “superhydrophilic” surfaces in SCIE (Science Citation Index Expanded) journals from 2000 to 2016.

1.2 Research purpose

Although the potential of wettability control for engineering metals is expected to be enormous, commercializing the related technology is still stagnant due to the issue of aging effect and derived problems. In case of fabricating superhydrophobic surfaces, superhydrophobic state realizes after passing several days from the day of surface structuring, which severely increase time cost as well as storage cost in mass-production stage. In case of fabricating superhydrophilic surfaces, it is difficult to achieve superhydrophilic state without chemical treatment, which limits the applications of wettability control technology. Therefore, it is urgent to define the existing problems, tackle them, and find effective solutions to accelerate commercializing the wettability control technology for engineering metals.

The purpose of this research is to investigate aging and heat treating effect on the wettability of stainless steel, one of the most widely used engineering metals in a wide range of industry, and to demonstrate wettability control for stainless steel surface without chemical treatment in consideration of aging and heat treating. This supports the feasibility of scalable fabrication process for superhydrophobic and superhydrophilic engineering metal surfaces, promoting the commercialization of wettability control technology for engineering metals.

1.3 Dissertation overview

In chapter 2, theoretical background of wetting and wettability on the engineering metals is introduced. The basic perspective of wetting on three-phase system (phase I: solid, phase II: liquid, phase III: air) is presented with wetting models for an ideally flat solid and a rough solid.

In chapter 3, aging effect is investigated by demonstrating time-dependent change of wettability against water on a flat stainless steel surface to define the phenomenon. The influence of oxygen for aging effect is explained to be a main factor.

In chapter 4, heat treating effect is investigated on a flat stainless steel surface. Effect of heat treating time and temperature to intrinsic wettability is studied. With the result of long-term observation of heat-treated samples, heat treating effect of wettability tuning is suggested, which yields instantaneous hydrophobic state and long-term hydrophilic state depending on heat treating temperature.

In chapter 5, wettability control process is demonstrated using laser-beam machining, electrochemical etching (ECE) and heat treating. Superhydrophobic and superhydrophilic stainless steel surfaces are fabricated with consideration of aging

effect. Instantaneous superhydrophobic state and long-lasting superhydrophilic state on the stainless steel surface are realized by heat treating.

In chapter 6, conclusion is presented with summary of the research and outlook.

2. Wettability

2.1 Surface free energy and surface tension

Understanding the wetting phenomenon of a liquid on the surface of a solid begin with surface free energy and surface tension. The concept of surface free energy and surface tension are fundamental in various fields from solid physics to surface engineering. Surface tension is the net intermolecular force on the surface of a liquid. Surface free energy is energy required to create a new surface. Both are closely correlated concepts; in the thermodynamic perspective, the concept of surface free energy is applied, whereas surface tension is used in the mechanical point of view originated from intermolecular force of a liquid. They should be comprehensively understood to further exploit them to control the wettability of a solid.

Surface free energy (J/m^2) is defined as the work per unit area by the force creating a new surface, quantifying the disruption of intermolecular bonds when a new surface is created. Cutting a solid body into pieces can be a good example to help understanding the concept. To cut a bulk sample, work is required, which is converted into new surfaces of bulk if assuming reversible process. In a more detail,

cutting a solid into two pieces disrupts the intermolecular bonds comprising the solid. If the cutting is done reversibly in an ideal case, the energy, or the work done by the cutting will be equal to the energy which the two new surfaces have. Eventually, the surface free energy of the solid is the half of the energy of cohesion of the solid.

Surface tension (N/m) is defined as the force tangent to the surface and normal to the dividing line between two systems. It is usually referred in case the system of interest is liquid. The origin of surface tension is explained by the force imbalance of intermolecular interaction. The attractive and repulsive interaction among molecules is omnidirectional, sharing with all neighboring molecules comprising the liquid, resulting in net force of zero. On the other hand, the molecules on the top of the surface don’t have identical molecules outward and therefore they are pulled inward due to an imbalanced intermolecular force. The shape of water droplet is the result of the surface tension, where water molecules on the surface is pulled into a spherical shape by the net force originated from the imbalanced intermolecular force.

The concept of surface free energy and surface tension can be summarized and easily understood by adapting the virtual work principle.[33] This intuitively accounts for the direction of surface tension which should be accepted to further

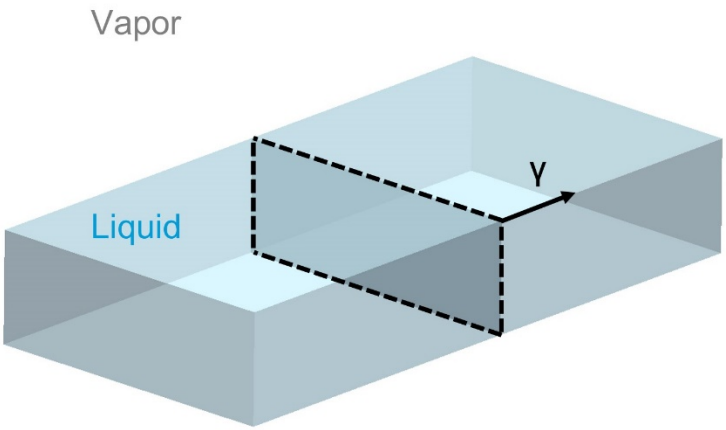

Figure 2.1 Schematic illustration showing surface tension (γ) as a force per unit length exerted by one subsystem on the other subsystem. Dotted line represents the virtual dividing line between the two subsystems in the liquid phase.

expand the theoretical explanation about wettability. Figure 2.1 shows the virtual model of a fluid bulk at rest divided by the dividing line of two subsystem crossing the liquid-vapor interface on which surface tension γ works. Here, it is postulated that two subsystem exert a repulsive force on each other, which is known as pressure, and surface tension is an attractive force acting on the interface, contrary to the pressure. The net force is proportional to the width W of the dividing line between the two subsystem. Assuming that one moves the dividing line by a length of dl, a new interface is created and the area is Wdl. This leads to the increase of free energy whose amount corresponds to γWdl. This energy increase should equal to the work done by the surface tension, which confirms that net force of surface tension is parallel to the interface, vertical to the dividing line, and have a magnitude of γW. Considering the net force per unit length, it is calculated to be γ, which corresponds to the surface tension which is postulated in the beginning of explanation. In this way, virtual work principle gives a brief notion about the link between thermodynamic and mechanical perspectives and it can be summarized that surfaces have a specific energy (surface free energy, or surface tension), which is originated from the cohesion of the underlying molecules constituting the phase.

2.2 Wettability of flat solid surfaces

Wetting refers to the ability of liquid to make contact with a solid surface. It is normally considered in three-phase interfaces comprised by liquid, solid, and gas. In this dissertation, wettability refers the degree of wetting of liquid water on a solid (engineering metal) surface surrounded by air. It differs depending on the combination of phases and two extreme cases can be presented to explain the boundary, as can be seen in Figure 2.2: 1) perfect wetting 2) non-wetting.[34] Perfect wetting is the behavior of liquid to make contact with a solid spontaneously to form a film. Non-wetting, on the other hand, describes a drop staying spherical without making contact to a solid surface. In the view of solid material, perfect wetting is the tendency of a solid to attract a liquid to substitute the solid/gas interface with the solid/liquid interface. This is described as superhydrophilic state. Non-wetting is a tendency of a solid surface to repel a liquid from being wet, maintaining solid/gas interface. This is described as superhydrophobic state.

Wettability of a solid, which is favorable of either being wet or non-wet is determined by the equilibrium among surface tension.[35] The fundamental concept can be first established for an ideal system comprised of solid, liquid, and air which are perfectly flat and chemically homogeneous. We call surface tension

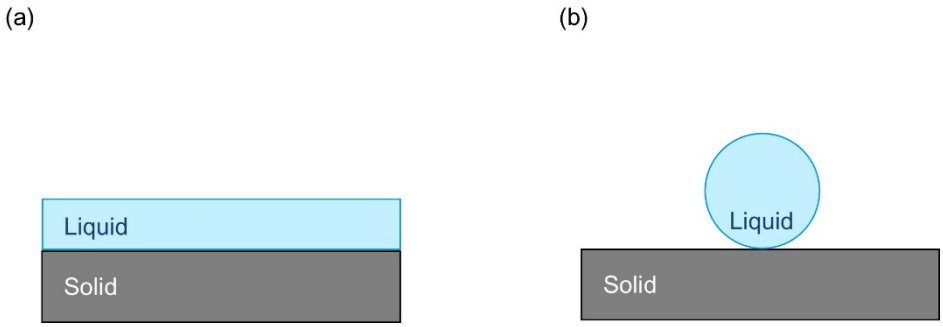

Figure 2.2 Schematic illustration of two extreme cases of wettability: (a) perfect wetting (b) non-wetting

of solid/liquid as γ_{SL}, solid/air as $\gamma_{SA,}$ and liquid/air as γ. As shown in Figure 2.3a, in case of wetting in which liquid forms a thin film on the solid, it can be explained by the balance among surface tensions where the sum of γ_{SL} and γ is larger than γ_{SA}. On the other hand, liquid will form a dorm shape on the surface and a contact angle θ will be developed at the interface where solid, liquid, and air meets by the force balance among γ_{SL}, γ_{SA}, and γ.[36] As presented in Figure 2.3b, the balance can be established as

$$\gamma_{SA} = \gamma_{SL} + \gamma \cos\theta. \quad (1)$$

The contact angle θ is thus determined explicitly by the intrinsic surface tensions originated from chemical nature of the different phases. Therefore, θ is referred as chemical angle in this dissertation.

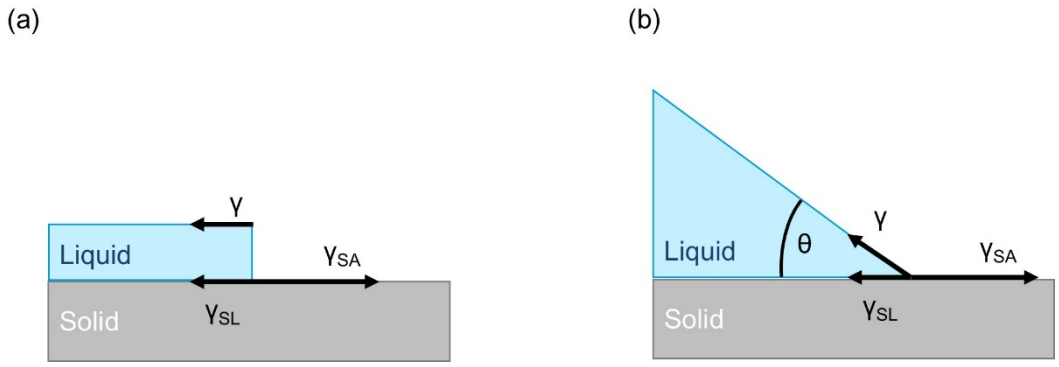

Figure 2.3 Two representative wetting cases for an ideal solid: (a) perfect wetting where a liquid fully spread on a solid (b) partial wetting where a liquid forms a contact angle θ at the three-phase interface determined by the balance of surface tensions

2.3 Wettability of rough solid surfaces

Contrast to the preceding explanation based on an ideally flat solid surface, most solid materials have roughness on the surface. Although macroscopically flat, surfaces in the real world are still rough at least in atomic scale. For example, solid materials made from the compaction of grains have the surface roughness at the scale of grains. Machining processes which removes the solid bulk materials by cutting or melting derives striations or microgrooves on the machined surface. Chemical coating which seems to generate a flat surface in naked eyes may have roughness which is originated from dewetting of the coating film. Therefore, the effect of roughness of solid surface should be considered to discuss wettability control.

There are two common models explaining the roughness effect on the apparent wettability which one can observe and measure: 1) Wenzel model, 2) Cassie-Baxter model. Both models support the feasibility of wettability control by surface structuring of solid materials.

Wenzel model explains the relationship between surface roughness and wettability.[37] Figure 2.4 shows a liquid drop on a rough surface spreading until the equilibrium. The rough surface is characterized by the roughness factor r, which

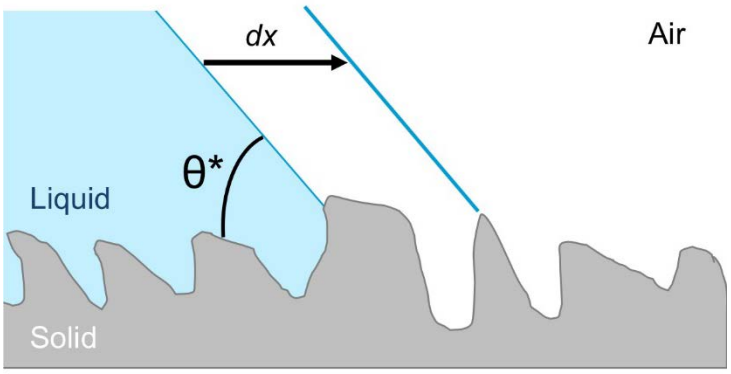

Figure 2.4 Schematic illustration of Wenzel model. Apparent contact angle (θ^*) is determined by considering a minute displacement (*dx*) of the contact line and the corresponding surface energy change with the assumption that the liquid fully spread on the surface following the profile of the roughness.

is the ratio between the actual surface area to the projected surface area. The contact angle θ^* (apparent angle) in the figure is presumably different from chemical angle θ which is determined by equation (1). Here, it is assumed that as the contact line progresses in the direction of *dx*, liquid totally conforms to all the surface roughness so that preexisting solid/air interface is fully substituted with liquid/air interface. In this situation, the difference of surface free energy *dE* can be calculated in terms of roughness factor and surface energy per unit length as

$$dE = r(\gamma_{SL} - \gamma_{SA})dx + \gamma dx \cos\theta^* \tag{2}$$

where the first term on the right hand side means the substitution of solid/air surface with solid/liquid surface and the second term means the creation of liquid/air surface as the liquid progress with a displacement of *dx*. The equilibrium $dE = 0$ yields the relationship between θ and θ^* by substituting equation (2) in (1),

$$\cos\theta^* = r\cos\theta. \tag{3}$$

The Wenzel model shown in equation (3) explains that roughness enhances wettability. In case of water droplet on a solid surface characterized by roughness factor *r* larger than 1, a hydrophilic solid ($\theta < 90°$) becomes more hydrophilic ($\theta^* < \theta$) and a hydrophobic solid ($\theta > 90°$) becomes more hydrophobic ($\theta^* > \theta$). This qualitatively implies the possibility of fabricating superhydrophobic surfaces with hydrophobic materials or superhydrophilic surfaces with hydrophilic materials by modifying surface roughness.

In Cassie-Baxter model, wetting of a liquid on a rough surface can be explained, especially for the superhydrophobic state originated from complex hierarchical structures in micro/nanoscale as can be found on lotus leaves.[38] While it is conceptually similar with Wenzel model, the difference is that liquid does not conform to the contour of the roughness. The liquid on the rough surface is partially supported by air trapped among cavities, as shown in Figure 2.5. Liquid is progress in the direction of *dx*, and the air keep trapped in the cavities of the roughness supporting the liquid not to touch the solid surface. In this situation, there are two different cases where liquid lies: 1) on the solid surface, 2) on the air surface. It can be assumed that the fraction of liquid lying on the solid surface is f_s and lying on the air is f_v, respectively, then the sum of f_s and f_v 1.[39] By substituting Cassie-Baxter equation in terms of f_s, f_v, and r, the relationship between apparent contact angle, fraction of wetting state, and roughness is obtained as

$$\cos\theta^* = rf_s \cos\theta + f_s - 1. \quad (4)$$

Cassie-Baxter model in equation (4) suggests that if fs is small enough, θ^* approaches to 180°, regardless of the chemical nature of the solid surface. In the wettability control point of view, this supports the feasibility of superhydrophobic metal surface by careful surface structuring without chemical treatment.

Wettability control is achieved by understanding the intrinsic wettability exploiting the roughness effect. In this point of view, Wenzel and Cassie-Baxter

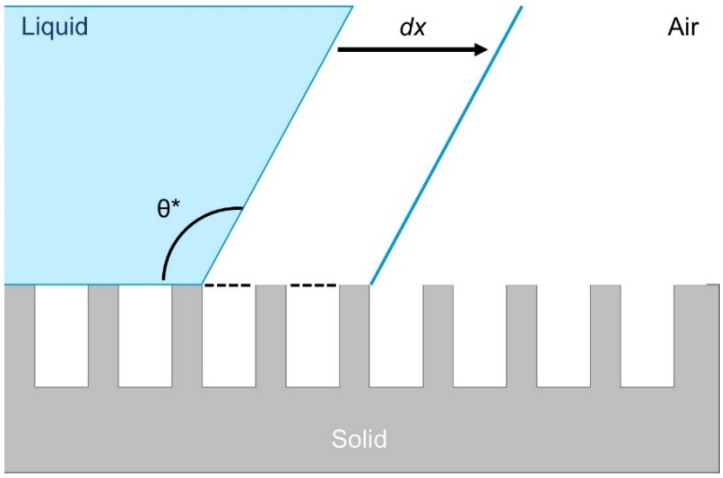

Figure 2.5 Schematic illustration of Cassie-Baxter model where a liquid does not follow the profile of surface roughness, but is supported by trapped air in the cavities on the rough surface. The energy balance due to the displacement (*dx*) of contact line includes the creation of liquid/air interfaces described as the dotted line.

which is characterized by chemical angle θ and structuring the surface in a way of models comprehensively explains the core concept of wettability control. Figure 2.6 shows the plot of Wenzel and Cassie-Baxter model. This plot visualizes two key points. First, intrinsically hydrophilic solid surfaces can be tuned to be hydrophilic or hydrophobic depending on geometric conditions and wetting state. Second, intrinsically hydrophobic solid surface only can be tuned to be more hydrophobic. Therefore, it can be summarized that wettability is determined by chemical factors (surface free energies) and physical factors (surface roughness) and the result of wettability control is predictable if information on chemical factor, which is quantified by chemical angle θ, is given.

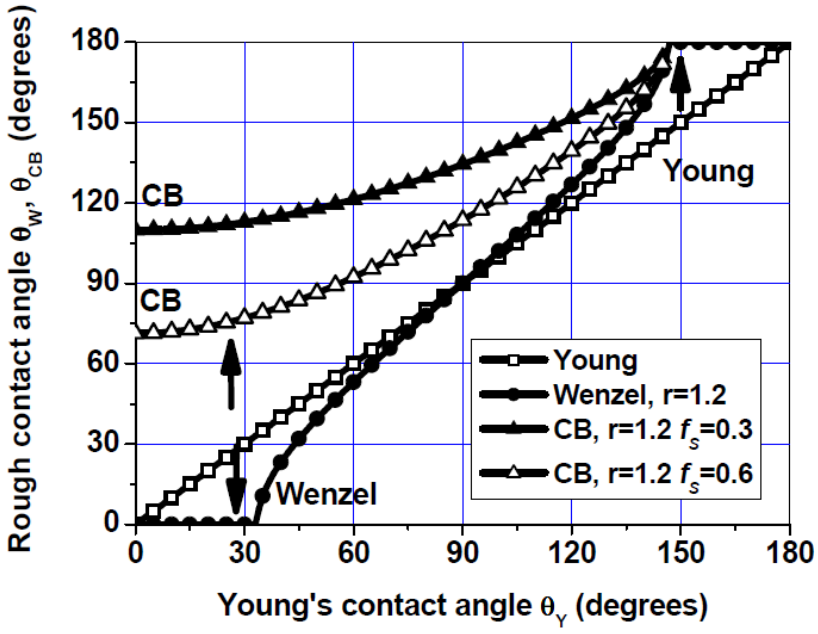

Figure 2.6. Theoretical relationship between chemical angle (Young's angle) and apparent angle (rough contact angle) of Young model, Wenzel model, and Cassie-Baxter model.[39]

2.4 Metal surfaces in the perspective of wettability

The surface of a solid metal is subtle to fully understand in the perspective of wettability. While the surface of metals is found to be generally hydrophilic which is prepared in a strictly-controlled manner,[40-42] it is still difficult question to define the wettability of metal surfaces in the real world. This is because of the structural and chemical complexity of metals and their alloys.[43] The nature of the layers depending on the composition and the processes to prepare bulk metal. It is worth noting that an oxide layer exists on top of the metal surface, which would greatly affects the wettability of a solid metal because it is the outermost layer directly interacting with external matters. Representative examples of metals possessing oxide layers on top of the surface are such as:

1) iron (Fe) whose surface layer is composed of iron oxides such as FeO at the near of a metal substrate and Fe_3O_4 and Fe_2O_3 on top of the surface, all of which is generally called as rust on the metal substrate

2) aluminum (Al), which develops oxide layers instantly after exposed to the ambient air, having an amorphous layer of Al_2O_3 and hydrated, thick, porous aluminum oxides on top of the surfaces.

3) Copper, whose initial appearance is shiny and bright, developing a layer of Cu_2O and CuO which results in dark and dull color.

From this fact, it can be inferred that the wettability of metal surfaces which is characterized by contact angle actually represents the wettability of the comprehensive state of surface consisting of diverse phases including metal oxides and adventitious moieties from an environment.[41]

In case of alloys, the heterogeneity of the surface becomes larger. Stainless steel is a good example which is one of the most widely used metal alloys. The corrosion-resisting feature of stainless steel is known from the passivation layer on the top of the surface, which a chemically different oxide layer compared with the outermost oxide layer of iron.[44] The oxide layer of stainless steel is found to be composed of a mixed phase of chromium oxides and iron oxides and the relative composition can be investigated by depth profiling using electron microscopic technology. However, it is still hard to discretely define the chemical composition of metal surfaces in situ.[45-46] The distribution of different phases on a stainless steel surface is very complex and irregular depending on the position. This hampers one from understanding the surface of metal alloys, and further expand it in the perspective of wettability. Therefore, understanding of metal surfaces in terms of wettability is extremely challenging, especially in case of surfaces of metal alloys. This is one of major challenges in the academia which is need to be shed light on

by extensive researches in various fields from solid physics to surface engineering.

In addition, difficulty of measuring the individual effect of outermost surface prevents one investigating the wettability of metal surfaces. There has been a continuous effort to understand the surface of metals in the view of wettability in a well-controlled experiment environment. Because of compositional complexity of alloys, attention has been focused on pure metals whose chemical composition uniform and homogeneous. This will help preparing a stable and well-characterized surface. An interesting phenomenon is observed that aging effect exists on the wettability of metal oxides. S. Takeda et al. demonstrated aging effect on the wettability of various metal oxides such as CrO_x, TiO_2 and ZrO_2 and suggested that the density of OH group on the surface eventually determines the wettability.[45] This reports may hint at the approach to investigate the surface of various engineering metals, yet there are still few reports to elucidate the fundamental aspect of engineering metals in the view of wettability.

In spite of such difficulties, there exists a need for technology of wettability control of engineering metals based on the expectation that wettability-controlled metal surfaces can yield an enormous commercial impact. To this end, it can be suitable to begin with focusing on providing solutions for controlling the wettability of engineering metals that can be directly applied to industrial use in an engineering perspective.

3. Aging effect on the wettability of stainless steel

Understanding substantive properties of a material is a fundamental requirement to exploit strong points of material properties for applications whose functionality can be significantly enhanced. A representative example can be found in the emerging field of surface science, seeking for a more suitable material to strengthen robustness and performance of wettability-controlled surfaces. Wettability-controlled surfaces based on controlling surface topography in micro/nanoscale have been ceaselessly presented with an attractive prospect of a higher value-added business;[47] however, the commercialization of related technologies is relatively stagnant due to the issues of durability.[48] Meanwhile, recent progressive development in microfabrication technology allows a variety of material selections for wettability-controlled surfaces.[8] In particular, commercial metals are still valuable up to today in the field of microfabrication because of various merits such as excellent mechanical properties, cost-effectiveness, a broad usability in a wide range of industry, etc. Accordingly, controlling the wettability

of metal surface has been gaining a growing attention in a recent few years, as a direct impact on the industry is expected.[7]

For functionalized metallic surfaces having controlled surface morphology, it is necessary to deeply investigate the essential characteristic of metal surfaces in the aspect of wettability. One of the related topics is the aging effect on the wettability of metallic surface – the time-dependent wettability transition from hydrophilic to hydrophobic property – and this has been drawing a lot of interest. Fabricating wettability-controlled metal surfaces involves various micromachining processes, which inevitably accompanies destructing a pre-existing surface layer and renewing the top surface. As the renewed surface interacts with various factors in the environments, the surface undergoes chemical/electrochemical reactions, which can be a main cause of the wettability transition. In recent works reporting wettability-controlled metal surfaces, several research groups observed time-dependent wettability transition on the surface.[21, 24-25, 27-28] There are several explanations finding the factors in the wettability transition of metallic materials. Oxygen[24-25], carbon dioxide[21], or organic matters in the atmosphere[27-28] have been proposed to be critical causes for the wettability transition of metallic materials mainly based on crystallographic approach. Yet, a more effort should be put to further expand our knowledge to understand diverse metal surfaces for utilizing them in a more practical manner. In particular, in case of alloy, it would

be more complicated to fully resolve the surface characteristics due to the material heterogeneity; therefore, in an engineering perspective, a more straightforward way should be used to study the surface characteristics.

In this chapter, aging effect is demonstrated on the wettability of AISI stainless steel 304 (STS 304) surface and identified that oxygen is the principal factor behind the effect. Subsequently, fabrication of microgrooved STS surface is demonstrated, which showed water-repellency without chemical surface treatment for applications exploiting the aging effect.

3.1 Experimental setup

The surface of samples were ground and polished with a grinder/polisher (Metaserv 2000, Buehler, Germany) to exclude the effect of surface roughness on the wettability in observation, as well as to renew the surface of STS 304 for the state of fresh surface just after being machined. While measuring static contact angle of a test liquid on the surface is a simple yet effective way of evaluating surface wettability, it does not fully indicate the wettability of material itself, but actually reflects apparent wettability in a strict sense. This is because roughness on the surface influences static contact angle; as is well known by the Wenzel model accounting for the relationship between the apparent wettability and the roughness of solid materials[37], apparent contact angle (θ^*) of the liquid is amplified by surface roughness (r), as

$$\cos\theta^* = r\cos\theta \tag{1}$$

where θ is intrinsic contact angle of the liquid determined on an ideally flat solid material.

Figure 3.1 shows the schematic illustration of the experimental procedure. Samples of 15 mm × 15 mm × 2 mm AISI 304 STS (STS 304, Nilaco Co., Japan) was ground to the depth of about 500 μm and finely polished to finish the surface.

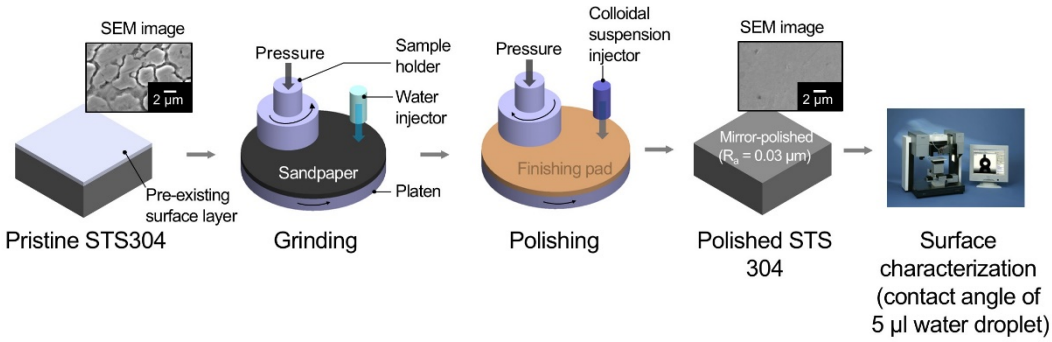

Figure 3.1 Schematic illustration of the experimental setup to characterize the wettability of STS 304 surfaces. Scanning electron microscope (SEM) images visualize the rough surface of STS 304 before polishing and flat surface after polishing.

Table 3.1 Chemical composition of stainless steel 304

Elements	Cr	Ni	Mg	Si	Ni	C	S	Fe
Weight %	18.00 ~ 20.00	8.00 ~ 12.00	2.00 max	0.75 max	0.1 max	0.08 max	0.030 max	Balance

A finished surface was measured with a profilometer (Form Talysurf Series 2, Taylor-Hopson, UK). The roughness average (R_a) of the finished surfaces was about 0.03 μm.

Table 3.1 summarizes a set of experiments to identify a dominant factor causing the aging effect. As oxygen and moisture are primary agents interacting chemically with the surface of metallic materials[49], the experiments were designed to detect individual effects of oxygen and moisture. Polished samples were stored in four different environments where the amount of oxygen and water is controlled. Case 1, where the sample was stored in an automatic nitrogen chamber, simulated the environments where the effects of oxygen and water are blocked. Case 2, where the sample was stored in a hermetically sealed container filled with deaerated deionized water, was mainly designed to see the effect of water, while the effect of oxygen was blocked. In Case 3, an airtight container was filled with deionized water without deaeration process and the sample was immersed in the container so that the effect depending on the amount of dissolved oxygen can be investigated. Finally, Case 4, where the sample was stored in a typical room condition, is for a combined effect of oxygen and moisture on the wettability of STS surface. All the cases were prepared in the same room.

Table 3.2 A set of experiments to investigate individual effects of oxygen and moisture

Case number	Description	Oxygen	Moisture
0	Initial state	-	-
1	Stored in a nitrogen chamber[a]	3 ppm	1 ppm
2	Immersed in deaerated deionized water[b]	1 ppm	submerged
3	Immersed in deionized water[c]	9 ppm	submerged
4	Stored in the ambient condition	2×10^5 ppm (~20 vol%)	1×10^4 ppm (RH ≈ 50%)

[a]The amount of oxygen and water is automatically controlled.

[b]Deaerated water was prepared by boiling it for 30 min and cooled down to room temperature.[50]

[b, c]Resistivity = 15 MΩ·cm

[d]Temperature = 20 °C

3.2 Demonstration of aging effect

Figure 3.2 presents the change of CA of water in the ambient condition for over 1000 days. Four polished samples were stored in a container and left in a typical room condition. Wettability was quantified by measuring CA of 5 μl deionized water with a drop shape analyzer (DSA100, Krüss, Germany). CA of water on each sample was measured every 24 hours. Presented data are average values of 10 measured CAs at random position. The initial CAs measured after the samples being polished were from 32° to 51°. In the first three days, we could observe a rapid increase in CAs of every sample near 80°. Afterwards, CAs tended to converge at a certain point about 85° in 7 days. We observed CAs to reach near 100° after 40 days from the initial state. The same samples were stored over 1000 days. CAs remain in the range from ~90° to ~100° after over 1000 days from the day of sample preparation. From the result, we could derive the conclusion that an initially hydrophilic STS surface becomes hydrophobic as time passes in the ambient condition.

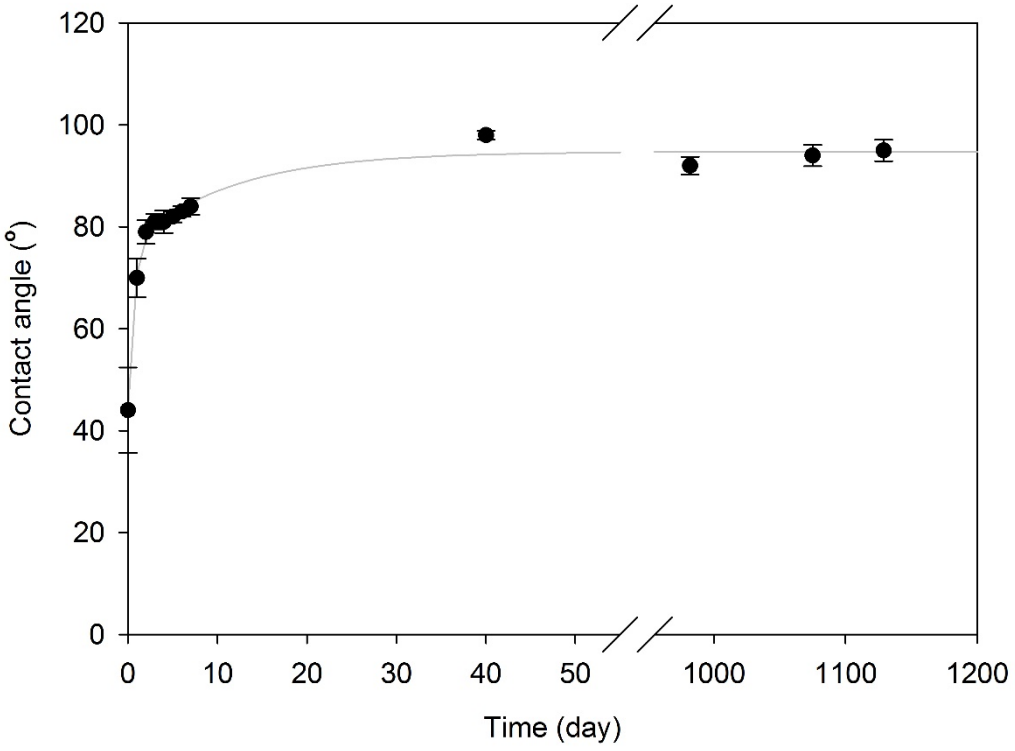

Figure 3.2 Change of static contact angle of water in the ambient air over 11 00 days.

3.3 Influence of oxygen on aging effect

As can be seen in Figure 3.3, the main factor behind the aging effect was identified to be oxygen from the change of CA of water in four different environments after 5 days from the initial state. Each sample was prepared and stored in a controlled environment as described in Table 3.1. First, we compared the results of Case 1 and Case 2 where the difference was in the existence of water. Because there was no significant difference in the CAs on both samples, we reached a conclusion that water in the environment has little effect on the wettability. Second, we correlate the results of Case 2 and Case 4 to see the effect of oxygen. We observed a noticeable difference in the CAs, implying that oxygen is directly related to the change of the wettability, whereas water did not show any correlation to the wettability. In short, the importance of oxygen and irrelevance of water to the wettability was verified from the two observations.

In addition, we examined the results of Case 2 and Case 3 where the amount of dissolved oxygen in deionized water was different. CA on the sample stored in the deaerated DI water was measured to be 60°, which was lower than CA of 68º on the sample stored in the DI water without deaeration. This result supports our inference in that CA increased as the amount of oxygen in the storing condition

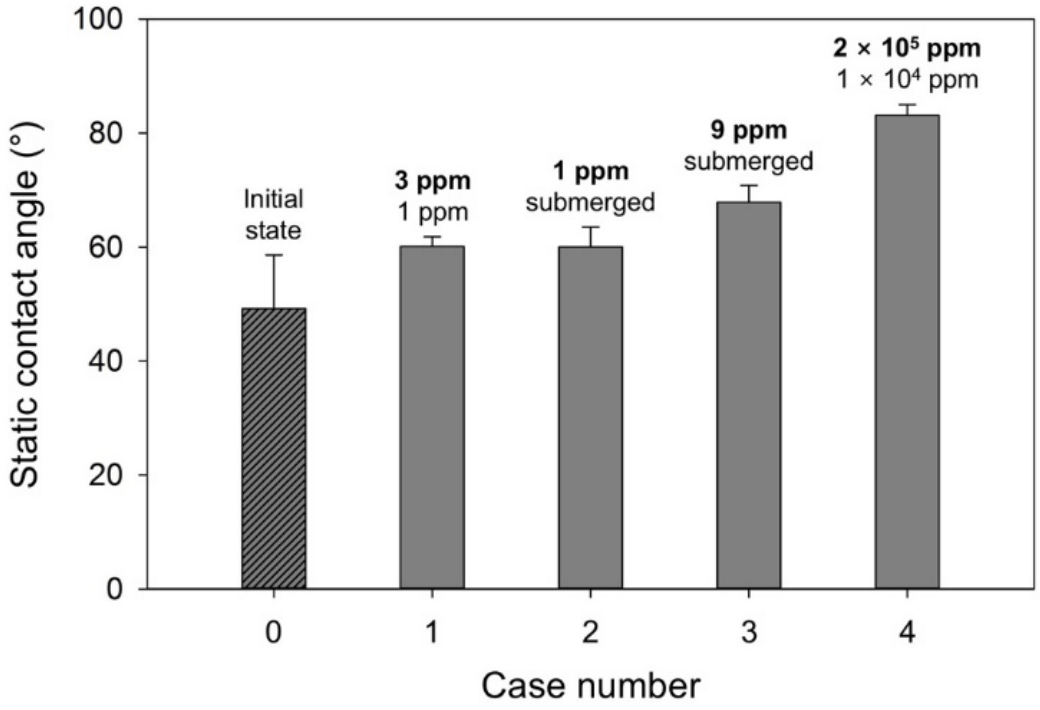

Figure 3.3 Change of contact angle of water on the samples stored in four different environments for 5 days (the amount of oxygen and moisture in each environment is presented in bold and plain text, respectively).

increased. Also, it implies that the bare STS surface reacted favorably with dissolved oxygen to reach a chemically stable state. As shown in the standard deviation of case 0, CAs measured on the fresh polished surface were relatively fluctuating, which displays instability of the surface. While measuring CA, the surface is exposed to the air and it readily begins forming initial passive film to some degree by a vigorous reaction with atmospheric oxygen. The surfaces of Case 1 and 2 could be considered to be at this state because large amount of oxygen was removed in each storing condition. Compared to the result of Case 2, the result of Case 3 suggests that the surface was in the middle of building a more developed passive layer, which would be chemically stabilized if a larger amount of oxygen is supplied as Case 4.

To further study the influence of oxygen, XPS (X-Ray photoelectron spectroscopy) analysis was conducted. XPS is one of the most surface-sensitive analytic methods to investigate the chemical state of a surface because the depth resolution of XPS is under 5 nm.[51-52] Figure 3.4 shows the results of XPS analysis (AXIS-Hsi, Kratos) for a fleshly polished STS 304 sample (labeled as “Day 0”) and a polished STS 304 sample stored in ambient air for 45 days (labeled as “Day 45”). The spectra shows peaks for O, C, Cr and Fe Table 3.2 presents the result of quantitative comparison of the atomic ratio between Day 0 and Day 45. The increase in the atomic ratio of oxygen was detected in Day 45, while the atomic

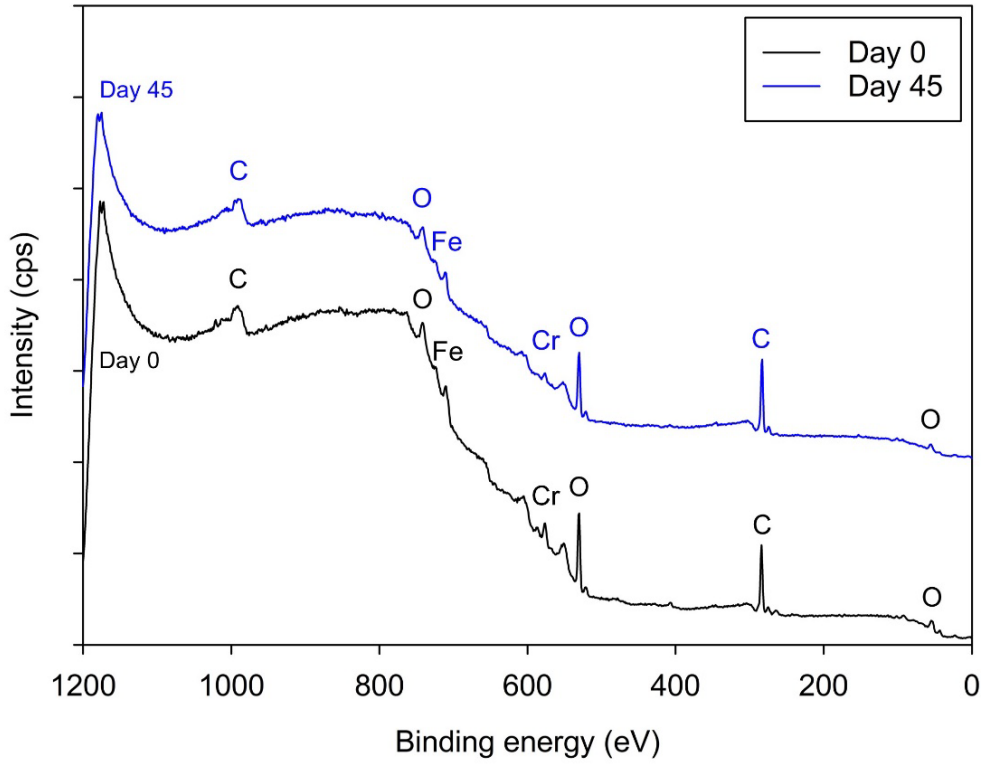

Figure 3.4 XPS survey spectra of freshly polished STS 304 sample and aged STS 304 sample in ambient air for 45 days.

Table 3.3 Elements in atomic ratios by XPS survey

Elements	Atomic %	
	Day 0	Day 45
O	77.9	82.7
Fe	12.9	12.4
Cr	9.2	4.9

ratio of Cr was decreased and the ratio of Fe remained similar. As shown above, the influence of oxygen was investigated by controlling the amount of oxygen in each storing atmosphere in Figure 3.3. The XPS result additionally supports that oxygen on the surface influences the wettability in a way of making surfaces hydrophobic.

XPS spectra of Cr 2p and Fe 2p in Figure 3.5 supports the explanation of aging effect in surface oxidation. Each spectrum in Figure 3.5 is deconvoluted by two curve fits, respectively. The curve fit on the right represents the chemical state of metal (lower binding energy, active species) and the curve fit on the left represents the chemical state of oxides and hydroxides (higher binding energy, less active species). By comparing the two curve fit, the overall change can be interpreted. Figure 3.5 (a) and (b) shows the reduction in the amount of Cr(0), which corresponds to the second peak at around 575 eV. The main peak of Cr 2p is at around 577 eV, which corresponds to the chemical state of chromium oxides. This suggests that Cr(0) on the freshly polished STS 304 reacted with oxygen in the atmosphere to form chromium oxides such as Cr_2O_3 or CrO_2. Figure 3.5 (c) and (d) also supports the chemical transition of Fe(0) to Fe(II) and Fe(III). The second peak at around 707 eV remarkably reduced and accordingly, the relative ratio of oxides to pure metal increased as the polished sample is stored in the ambient air. From this result, it can be concluded that the aging effect can be explained in the transitional oxidation state of the surface and the complex mixture of oxides on the

Table 3.4 Binding energy of the chemical states of Cr 2p and Fe 2p spectra [53-55]

Element	Chemical state	Binding energy (eV)
Cr 2p (chromium)	Cr(0) (metal)	574.1
	Cr(III) (oxide)	575.7, 576.7, 577.5, 578.5
	Cr(III) (hydroxide)	577.3
	Cr(VI) (oxide)	579.6
Fe 2p (iron)	Fe(0) (metal)	706.8
	Fe(II) (oxide)	709.5
	Fe(III) (oxide)	710.0, 711.0, 711.9, 713.0, 714.1
	Fe(III) (hydroxide)	713.2

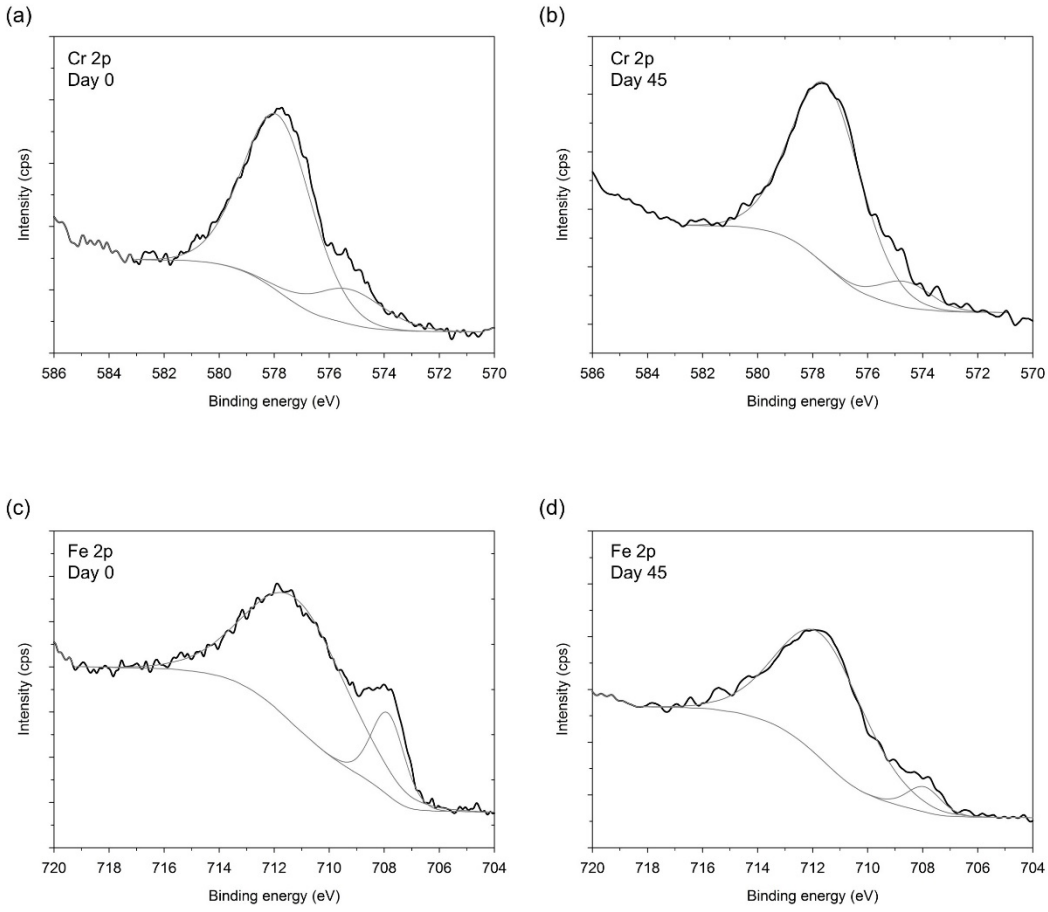

Figure 3.5 XPS spectra of Cr 2p of (a) Day 0, (b) Day 45 and Fe 2p of (c) Day 0, (d) Day 45.

surface eventually lead to the hydrophobic surface in the view of wettability.

3.4 Superhydrophobic stainless steel utilizing aging effect

Figure 3.6 shows an example utilizing the aging effect that water-repellent STS surface can be made without any chemical surface treatment. The depth and the width of groove was 200 μm and 500 μm, respectively, and the detail fabrication procedure can be found elsewhere. [18] As can be seen in Figure 5a, we initially observed superhydrophilicity on the surface just after fabricating the sample. After storing the fabricated sample in the ambient condition for 30 days, however, we found 5 μl water droplet stay on the surface with the contact angle of 161°. Here, it is worth noting that there was no artificial surface treatment such as chemical coating with low-surface-energy materials. Considering the potential usefulness and the impact of such functionalized metallic surface, it would be beneficial to find the method to accelerate the aging effect for a higher production yield.

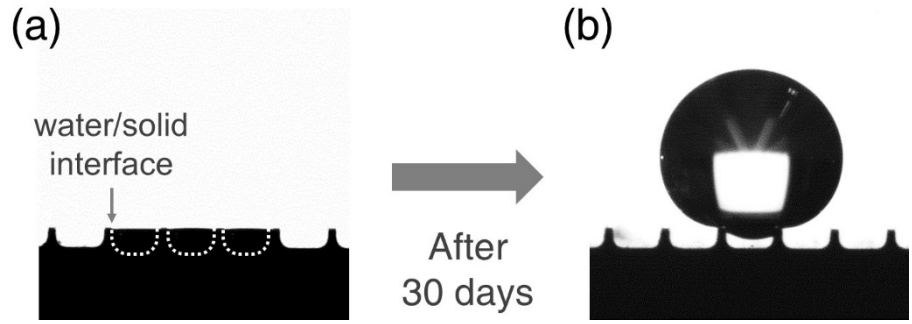

Figure 3.6 (a) Microgrooved stainless steel surface initially exhibited superhydrophilic wetting property just after being machined. (b) After 30 days, the same surface showed superhydrophobic characteristics, with the contact angle of water droplet of 161°.

4. Heat treating effect on the wettability of stainless steel

Aging effect is not only inevitable in the fabrication process, but also problematic in wettability control of engineering metals, as mentioned in Chapter 1. Aging effect is critical in regards to scaling-up the related technology because it prolongs the duration of fabrication process for superhydrophobic surface. Also, eventual hydrophobic state of engineering metal surfaces limit itself from expanding the applications. However, little effort has been put to handle aging effect academically so far. Most of previous research recognized and observed aging effect, yet, it is still limited in that aging effect has not been regarded as a problem to be solved. [21, 24-31] While several explanations were given to account for aging effect, there has been little perspective of observing aging effect as a problem. In 2016, Chun et al. pointed out that the aging effect is problematic in the view of productivity of superhydrophobic metal surfaces.[19] They suggested heating metal samples at 100 °C can shorten the time required to fully develop the aging effect on the wettability.[19, 32] However, more effort should be put to further expand our knowledge for aging effect

Since the influence of oxygen on the aging effect was explained and supported by XPS result in Chapter 3, it can be a suitable approach to focus on oxidation on the surface to deal with aging effect. By changing ambient temperature after modifying the surface of stainless steel, it can be expected that the resultant oxides on the surface of stainless steel may vary. The difference in the oxidation state depending on temperature can result in the different wettability. This approach refers to heat treating of metals, which is a conventional method to enhance properties of engineering metals. By controlling heating temperature, heating time, and cooling rate, diverse mechanical properties such as strength, hardness, ductility as well as electrical properties or dimensional stability of products can be improved.[56] There is little information, however, about the relationship of heat treating and the wettability, though heat treating is highly likely to have an influence on the wettability.

In this chapter, heat treating effect on the wettability on stainless steel (type 304) is investigated. By changing the heat treating time and temperature for polished stainless steel samples, effective heat treating time and temperature is determined to modify the wettability. Two effects of heat treating is studied by observing the change of contact angle on heat-treated samples at different temperatures over 200 days.

4.1 Experimental setup

Figure 3.1(a) presents the schematic illustration of experimental procedure to investigate heat treating effect on the wettability of stainless steel. Pristine stainless steel (type 304, Nilaco Co., Japan) samples cut in the size of 15 × 15 × 1 mm^3 were mechanically ground and polished to flatten the surface as conducted in Chapter 3. Freshly polished samples were stored in a furnace (FT-830, Daihan Scientific Co. Ltd., temperature resolution = 1) set at different temperature and time for heat treating. The range of heat treating temperature was set starting from 50 to 400 °C. The maximum temperature is set to prevent sensitization of stainless steel (Figure 3.1(b)).[56] The range of heat treating time was set from 1 h to 48 h. After heat treating, samples were cooled down in ambient air. Contact angle (CA) of 5 μl of water droplet was placed on the surface of samples over 10 times at random position, deriving the average and the standard deviation of measured CA.

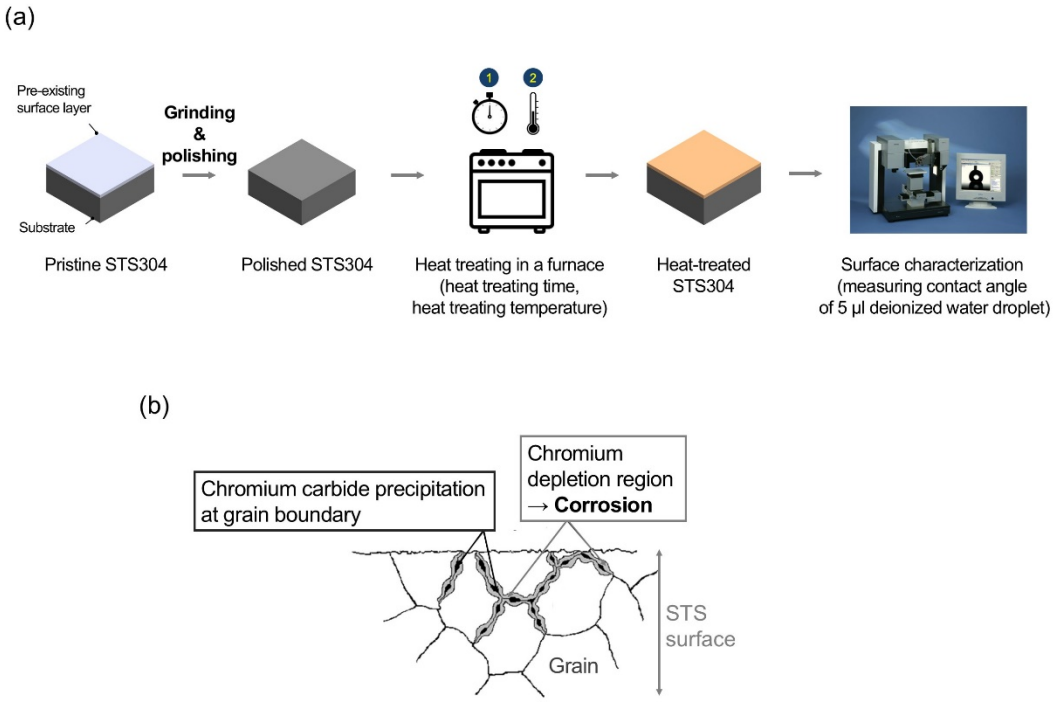

Figure 4.1 (a) Schematic illustration of experimental procedure to investigate heat treating effect on the wettability of stainless steel. (b) Schematic illustration of sensitization occurring in the heat treating of stainless steel at around 425 ~ 900°C.[56]

4.2 Influence of heat treating time

Influence of heat treating time on the wettability of stainless steel was investigated by varying the heat treating time from 1 h to 48 h. Here, the heat treating temperature was fixed at 50 °C and 300 °C, respectively.

Figure 4.2 shows that the effective heat treating time was 6 h to induce the significant change of wettability. Data on 0 h refer to contact angles measured as soon as samples were polished. Heat-treated samples at 50 °C displayed a proportional increase of CA from 1 h to 6 h and CA of 12 h, 24 h and 48 h remained similar in the range of 70° ~ 80°. Heat-treated samples at 300 °C also exhibit an increase of CA from 1 h to 3h, however, sudden drop of CA was observed at 6 h of heat treating. CA after 6 h stayed in the range of 10° ~ 20°. From this result, it can be concluded that wettability of stainless steel is influenced by heat treating and heat treating time should be set at least 6 h or more. To further investigate the heat treating effect, heat treating time was fixed at 6 h.

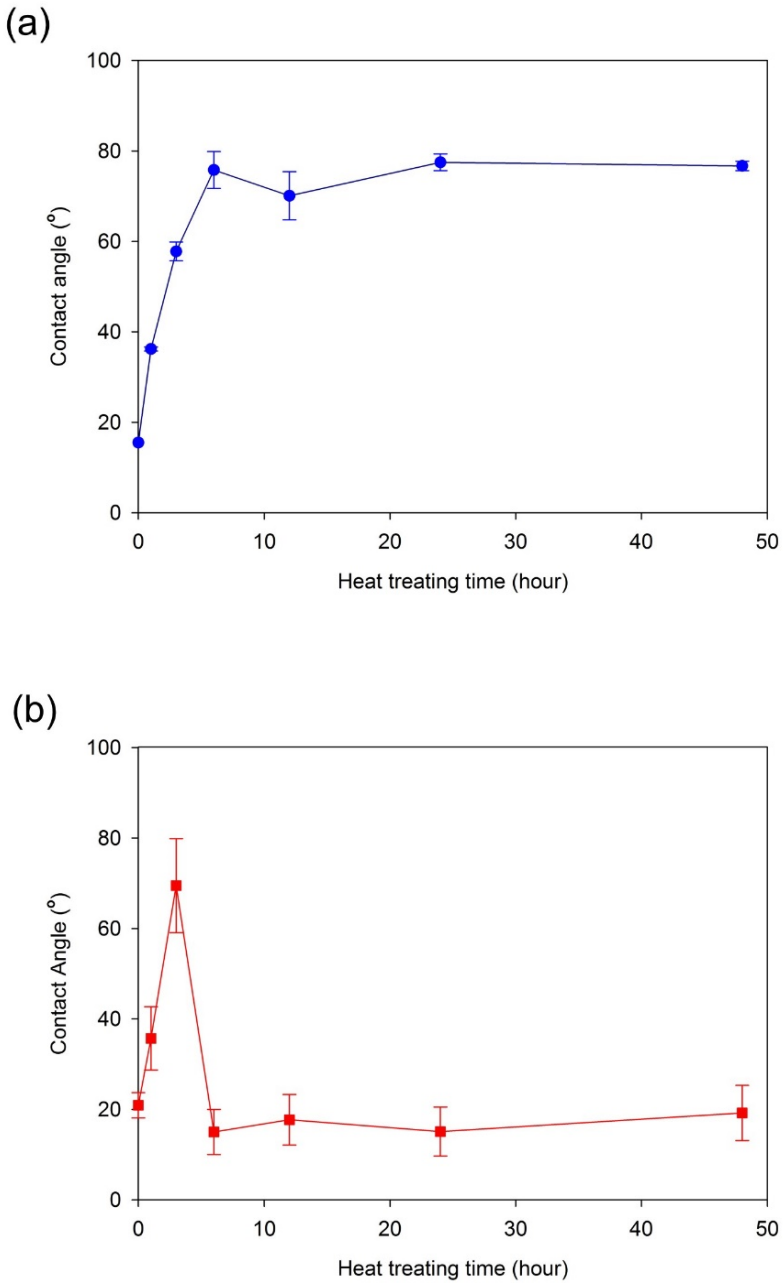

Figure 4.2. Change of CA measured on the samples heat-treated at (a) 50 °C and (b) 300 °C depending on heat treating time

4.3 Influence of heat treating temperature

Influence of heat treating temperature on the wettability of stainless steel was investigated by heat treating polished stainless steel samples at different temperatures for 6 h. Here, the heat treating time of 6 h was determined in 4.3.1. Temperature range was set from 50°C to 400°C and the temperature difference was set to be 20°C starting from 100°C to 300°C.

Figure 4.3 displays the change in CA after heat treating and the resultant CA after heat treating is distinguished three parts in overall: 1) 50 °C ~ 140 °C, 2) 160 °C ~ 260 °C, and 3) 280 °C ~ 400 °C. In the temperature range from 50 °C to 140 °C, the surfaces of heat-treated samples exhibit hydrophobic state. In this range, CA varied from 76° at 50 °C to 91° at 140 °C. In the temperature range from 160 °C to 260 °C, the surface displays minor increase in CA. Lastly, samples heat-treated over 280 °C demonstrated hydrophilic state whose CA is less than 20°.

The result in Figure 4.3 suggest that heat treating can be an effective method to deal with aging effect. Depending on the temperature range, resultant CA is significantly different, especially between the range of 50 °C ~ 140 °C and the range of 280 °C ~ 400 °C. Temperature from 50°C to 140°C results in hydrophobic surfaces, whereas temperature from 280 °C to 400 °C gave hydrophilic

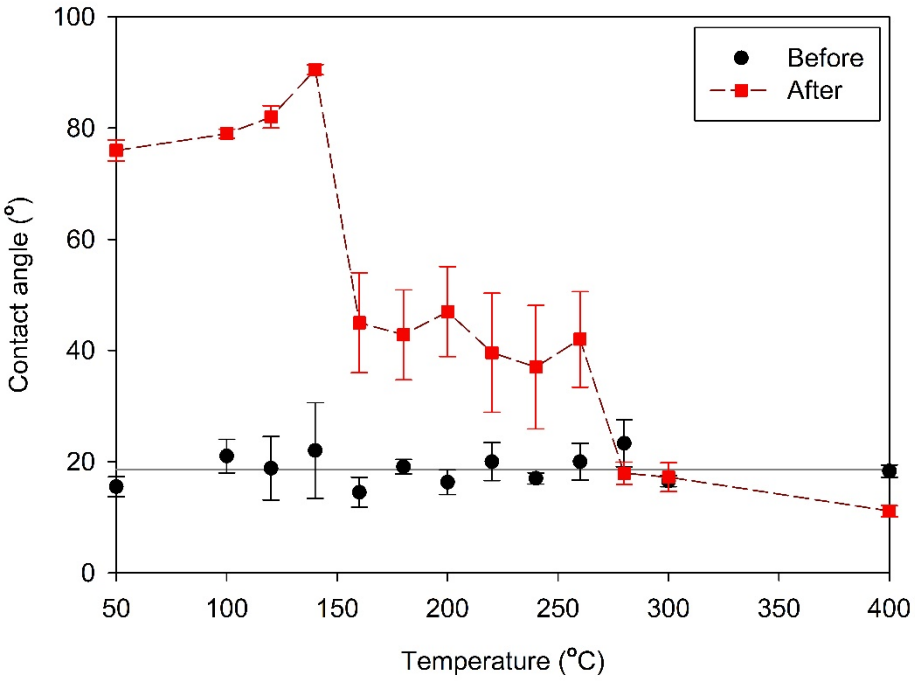

Figure 4.3 Change of CA before heat treating (labeled as “Before”) and after heat treating (labeled as “After”) in different heat treating temperatures from 50°C to 400°C for 6 h. Mean value of CA on freshly polished stainless steel surfaces was presented as grey line which are avaraged from 12 samples.

surfaces. Further observation is followed in 4.3.3 to investigate the change in CA of heat-treated samples after heat treating for over 200 days, which shows the final resultant wettability by heat treating.

4.4 Wettability-tuned stainless steel surface by heat treating

In Chapter 4.3, two significant temperature ranges, 50 °C ~ 140 °C for hydrophobic surfaces and 280 °C ~ 400 °C for hydrophilic surface, were explained and the feasibility of modifying the intrinsic wettability of stainless steel was suggested. To support this, two samples from each temperature range were selected: 1) heat-treated samples at 100 °C and 140 °C for hydrophobic surfaces 2) heat-treated samples at 300 °C and 400 °C for hydrophilic surface. CA was measured just before heat-treating (labeled as “Day 0”). Samples were stored in ambient air over 40 days and measured CA again (labeled as “Day 40”). This is to investigate the resultant wettability after heat-treating at respective temperature ranges.

Figure 4.4 shows the change in CA of heat-treated samples over 40 days, which shows aging effect on heat-treated samples. In Day 0, Sample 100 °C and 140 °C showed relatively hydrophobic state (CA ≈ 80° ~ 90°) compared to sample 300 °C and 400 °C demonstrating hydrophilic state (CA ≈ 10° ~ 20°) After 40 days, it is observed that there were a slight increase in CA of sample 100°C and 140°C and a relatively larger increase in CA of sample 300 °C and 400 °C. This suggests the aging effect on the heat-treated samples. When considering the final wettability, the result proposes that two different surfaces, hydrophobic and hydrophilic, were

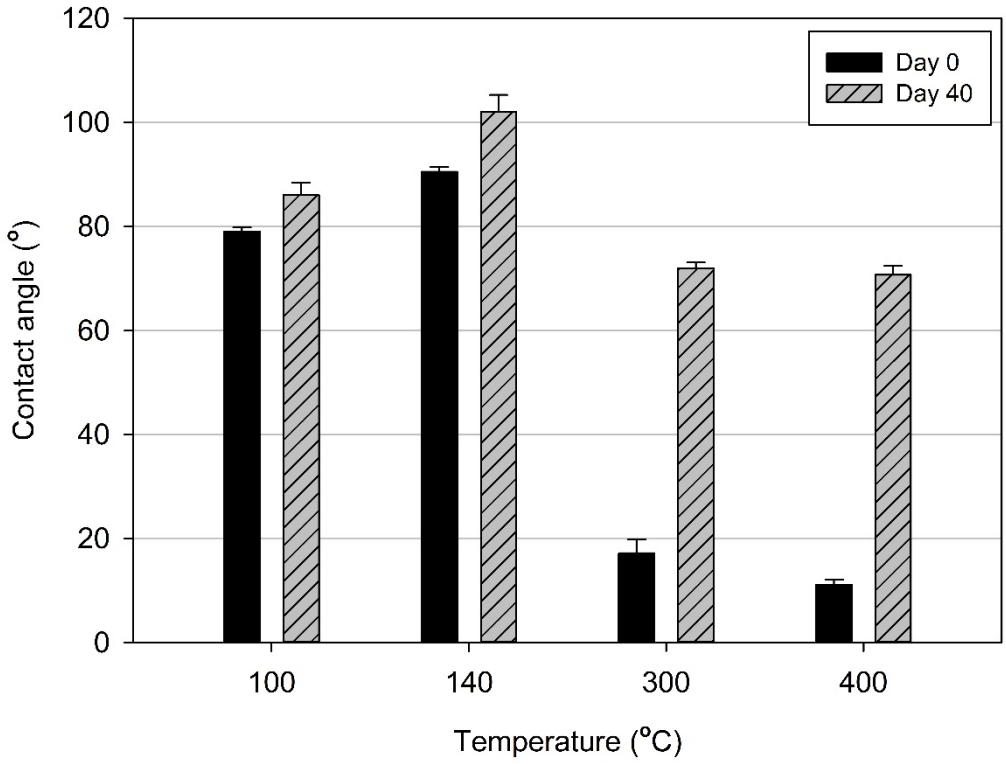

Figure 4.4 Change in CA of heat-treated samples at 100 °C, 140 °C, 300 °C and 400 °C stored in ambient air over 40 days.

achieved depending on the heat treating condition. Accordingly, a more detailed observation as well as chemical analysis was necessary to confirm the resultant wettability by respective heat treating temperature ranges.

It was confirmed in Figure 4.5 that heat treating at 140 °C for 6 h eventually yields hydrophobic surfaces. The change in CA after heat treating at 140 °C for 6 h was monitored for about 200 days and initial hydrophobic surface holds the wettability as time passes, with the final CA reaching 98°. Also, CA of initial hydrophobic surface is 91° which is measured just after heat-treating the sample. Additionally, the difference in CA in the first 6 days was only 6°, which suggests that the heat-treated surface at 140 °C is in a relatively stable state. This result proposes that heat treating at 140 °C for 6 h is to shorten aging time for hydrophobic surfaces. Resultant wettability of sample 140 °C after passing over 40 days corresponds to that of polished stainless steel stored in ambient air with final CA of about 95°. However, the difference can be found in the data of Day 0. While the CA of sample 140 °C in Day 0 is 91°, the CA of control in Day 0 is 44°. This can be interpreted that aging time of 40 days in ambient air is shorten to be 6 h just by heat treating at 140 °C. Therefore, it can be concluded that the heat treating effect at 140 °C, 6 h can be defined as a method to shorten the typical aging time which takes tens of days to just 6 h when hydrophobic surface is needed.

Figure 4.6 suggests that heat treating at 300 °C for 6 h realizes hydrophilic

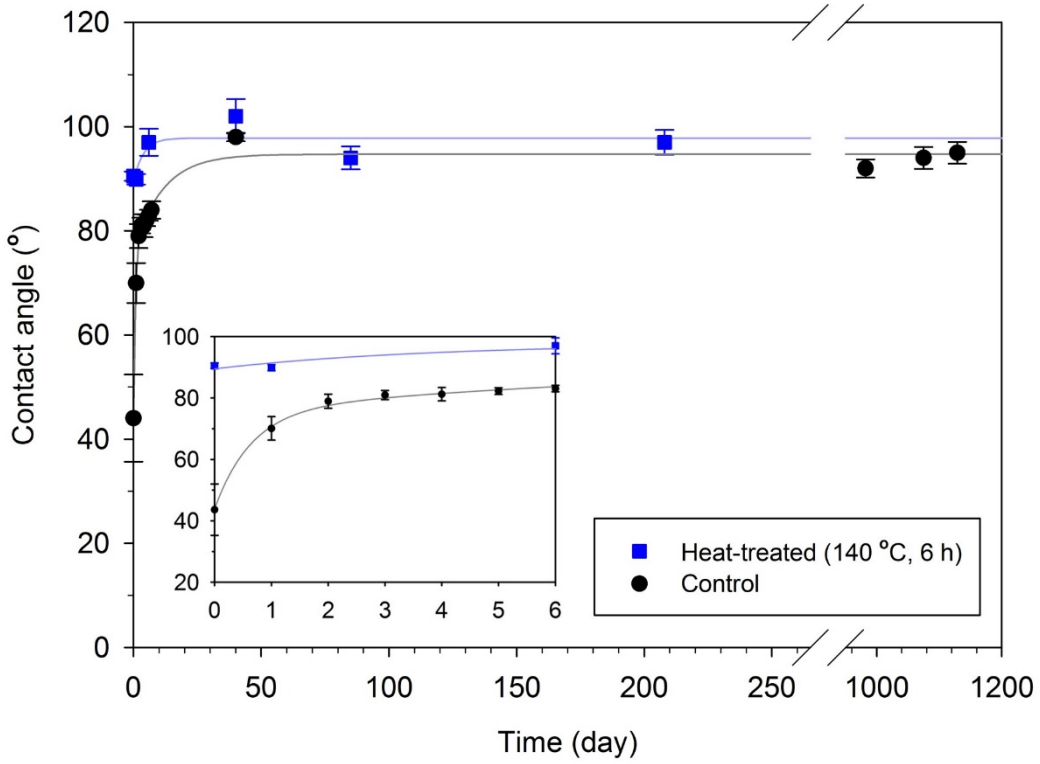

Figure 4.5 Change in CA of heat-treated (140 °C, 6 h) sample and control sample. Heat-treated stainless steel sample was compared with the data in Figure 3.2 (polished stainless steel without heat treating) as control. Inset shows the data from day 0 to day 6.

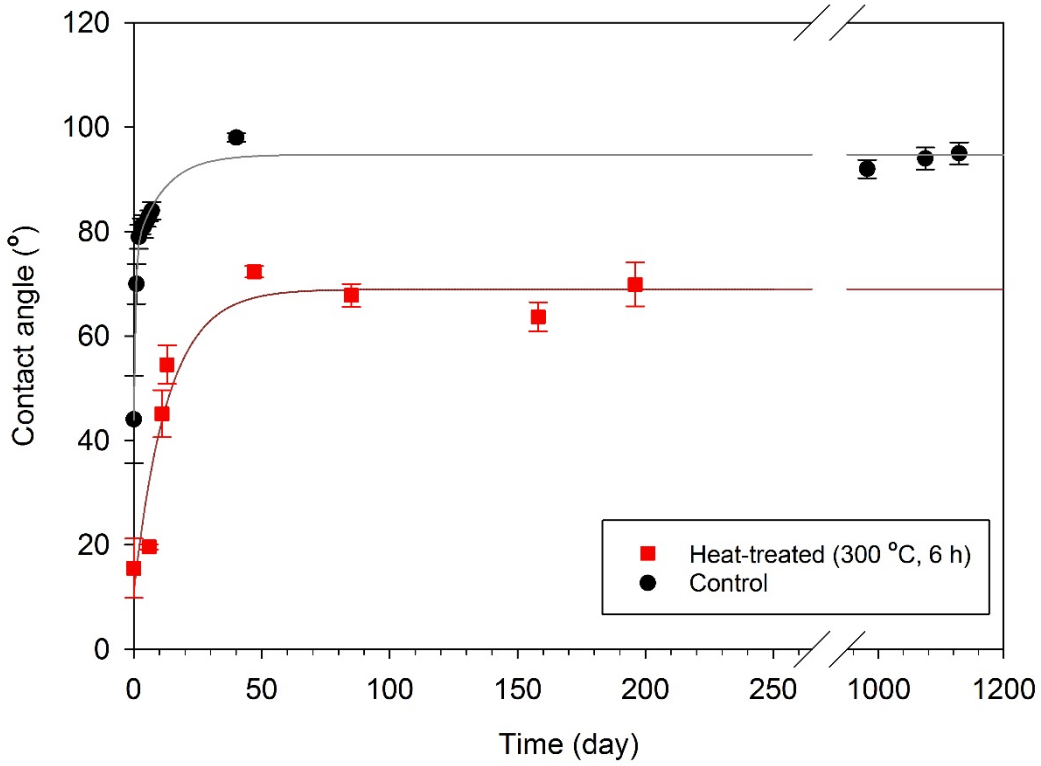

Figure 4.6 Change in CA of heat-treated (300 °C, 6 h) sample and control sample. Heat-treated stainless steel sample was compared with the data in Figure 3.2 (polished stainless steel without heat treating) as control.

stainless steel surface. In the first 40 days, CA in Day 0 rises from 16° up to 72°, showing a gradual increase in CA. This behavior was previously demonstrated in Figure 3.2 in Chapter 3, which corresponds to the rising behavior of CA from relatively hydrophilic state to hydrophobic state with final CA near 90°. Here, an interesting result is observed that CA stayed at around 70° after 47 days. From this point, the wettability remained constant for 200 days, exhibiting CA near 70° in Day 47, 85, 158 and 196. In comparison with control sample, it is remarkable that the final CA of sample 300 °C is smaller than that of control sample. This supports that hydrophilic surface is realized by heat treating polished stainless steel at 300 °C for 6 h. Therefore, it can be concluded that heat treating effect at 300 °C for 6 h can be described as a method to change intrinsic wettability of stainless steel to a more hydrophilic state. This would be enormously useful when fabricating hydrophilic surfaces with stainless steel, whose initial wettability become lost as time passes due to aging effect.

To investigate chemical change depending on heat treating condition, XPS analysis was conducted and the result is presented in Figure 4.7. First, the hydrophobic surface achieved by heat treating at 140 °C for 6 h can be explained by the surface oxidation. In Figure 4.5 (c), the relatively low signal intensity of iron and chromium metal region (binding energy = 574.1 eV for iron metal and 706.8 eV for chromium metal) suggests that the surface is readily oxidized after heat

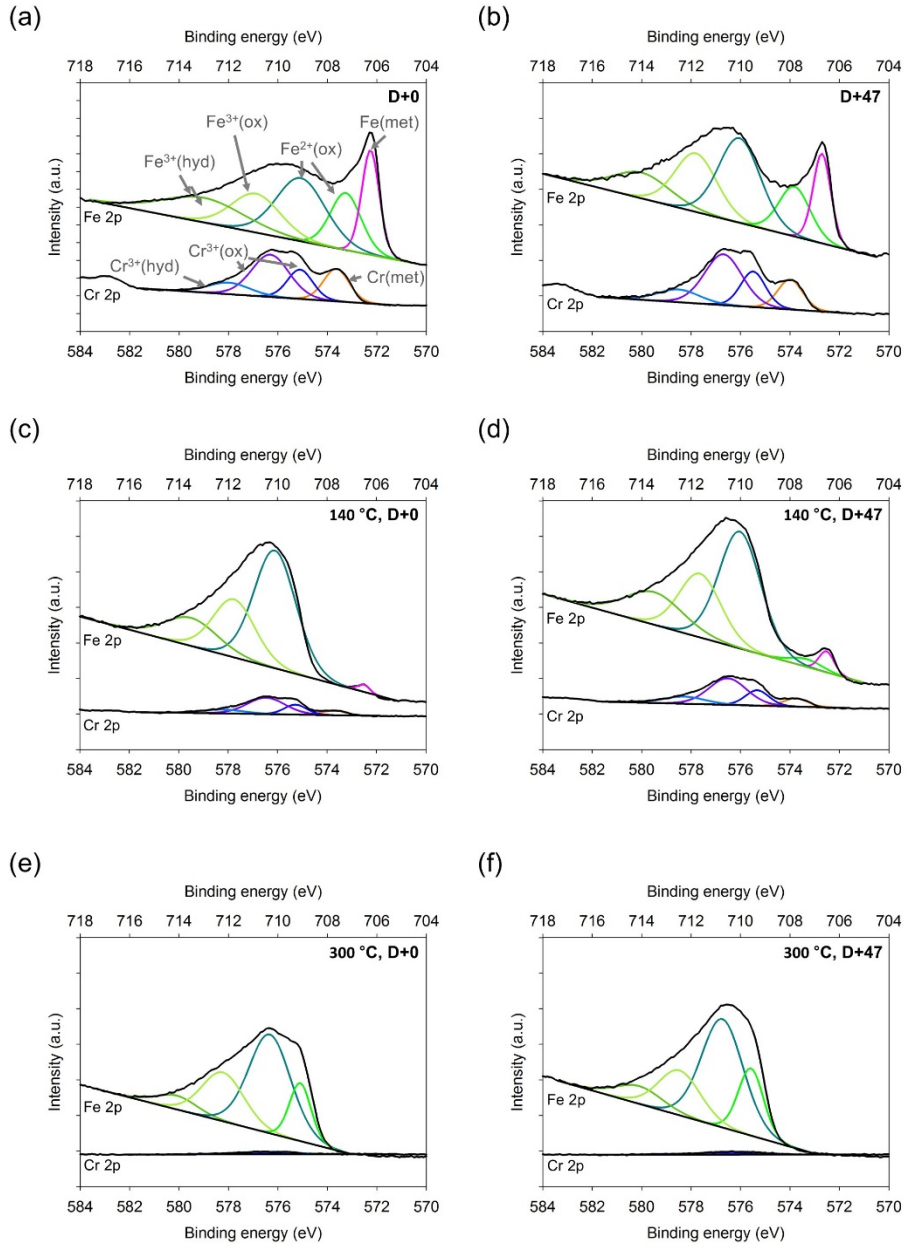

Figure 4.7 XPS spectra of Fe 2p and Cr 2p of (a), (b) polished STS samples and (c) ~ (f) heat-treated samples after being polished. Heat treating condition and aging time is written in each plot. (Refer to Table 3.4 for chemical states)

treating at 140 °C for 6 h, resulting in a complex mixture of various oxides and hydroxides dominating on the surface.

The hydrophilic surface achieved by heat treating at 300 °C for 6 h can be explained by the depletion of chromium in the outermost surface layer. In Figure 4.7 (e), while the spectra of Fe 2p shows the surface oxidation, the intensity in the spectra of Cr 2p is hardly observable. This suggests that chromium was depleted after heat treating. Chromium depletion by heat treating in air was observed in the previous research as shown in Figure 4.8.[57] It was found that the surface of heat-treated stainless steel 304 consists of mainly two distinguishable layers depending on the existence of chromium. Whereas chromium can be barely found at the outermost layer in the thickness of several nanometers, there is a significant amount of chromium in the inner layer. In Figure 4.7 (a) ~ (d), the spectra of Cr 2p can be found and the final contact angle of these surfaces reaches over 90°, which characterizes a hydrophobic surface. In contrast, in Figure 4.7 (e) and (f) which display chromium depletion at the outermost surface, the final contact angle is ~70°, which characterizes a hydrophilic surface. From this, it can be concluded that the existence of the chromium-related matters determines final wettability of the surface.

Aging effect on the heat-treated samples can be explained by change in the chemical composition of surfaces stored in the air. Comparing data presented in

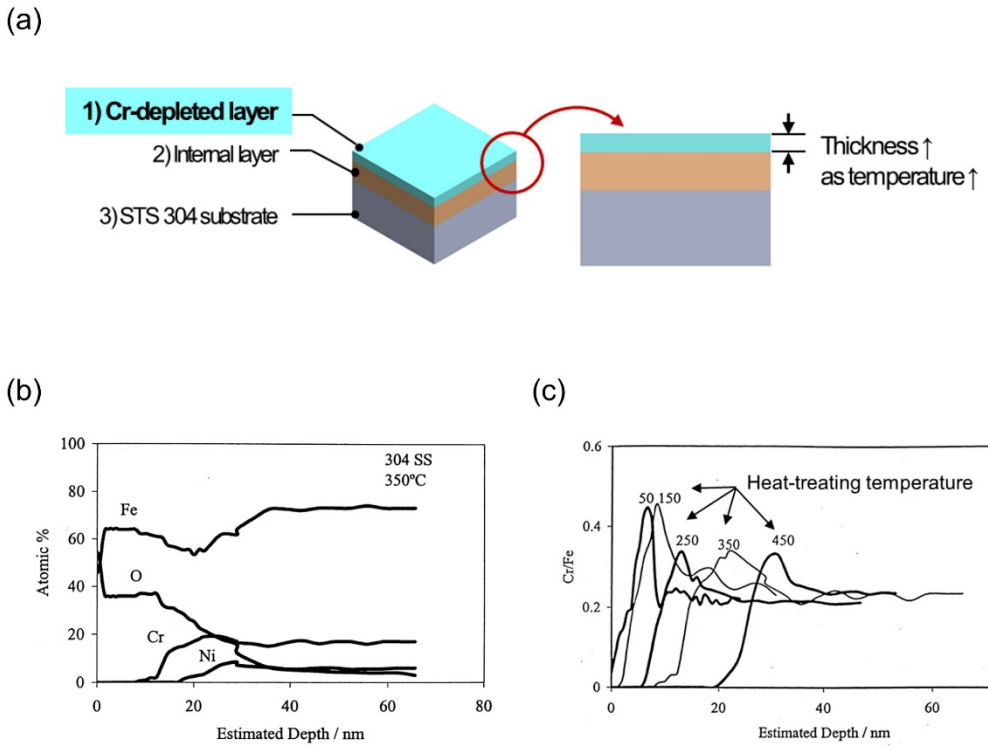

Figure 4.8 (a) Schematic illustration of heat-treated stainless steel surface structure depending on the amount of chromium. (b) Elemental composition of heat-treated stainless steel surface. Chromium is found beneath the outermost layer that is mainly composed of iron and oxygen. (c) Change of Cr/Fe ratio depending on the depth from the surface.[57]

Figure 4.6 (c) and (e) to (d) and (f), it can be found that there is a slight change in the spectra. This suggests that the surfaces chemically change while being stored in the air after heat-treating.

In a thermodynamic perspective, chemical change of the surfaces can be illustrated as oxidation of the top surface by reacting to the air and interconversion of the complex oxides at the surface layer transforming one to others.[58] It is well known that there are more than single possible reaction pathways for an oxide in a given oxic condition and atmospheric temperature plays a key role in determining a pathway of oxidation as well as kinetics. Also, stainless steel is composed of several chemical elements, which makes it even more difficult to quantitatively explain the change. Therefore, nature of oxidation of stainless steel surface is highly challenging to fully elucidate.

In spite of such difficulties, it can be briefly summarized that the surface changes ahead to the thermodynamically most stable states, Fe_2O_3 and Cr_2O_3, by simplifying the surface of stainless steel surface as Fe-Cr-O system and utilizing the concept of change in Gibbs free energy (ΔG). As presented in Table 4.1, the most stable state of oxides in Fe-O and Cr-O systems is Fe_2O_3 and Cr_2O_3 which are major end member of reaction pathways of iron and chromium oxidation.[59-60] Therefore, the surface change can be interpreted to be a thermodynamic progress to the equilibrium and the state of progress can be accelerated by heat treating.

Table 4.1 Representative oxidation reaction in Fe-O and Cr-O system at 500 K, 1 atm.[59-60]

Reaction	ΔG (kJ/mol)
Iron	
$Fe + 1/2O_2 \rightarrow FeO$	-112
$3Fe + O_2 \rightarrow Fe_3O_4$	-115
$3FeO + 1/2O_2 \rightarrow Fe_3O_4$	-125
$2Fe + 3/2O_2 \rightarrow Fe_2O_3$	-130
Chromium	
$Cr + O_2 \rightarrow CrO_2$	-477
$4/3Cr + 3/2O_2 \rightarrow Cr_2O_3$	-690

As a further study, it was investigated that additional heat treating on the hydrophilic STS surface achieved by heat treating at 300°C for 6 h results in a more hydrophobic surface readily. Figure 4.9(a) shows the initial CA and the change in CA of two different samples for the aging time of 40 days. As demonstrated 4.2 and 4.3, heat treating STS 304 in 300 °C for 6 h yields a hydrophilic surface with CA less than 20°. If an additional heat treating of 140 °C for 6 h is followed, the resultant surface become relatively hydrophobic with CA of 63°. By comparing the initial wettability with the resultant wettability after 40 days of aging time, it was found that aging effect in case of the additional heat treating is relatively minor compared to that of the hydrophilic STS surface.

While the difference in the wettability is significant between the two different heat treating condition, it was difficult to reveal the chemical difference among the surfaces solely by XPS analysis. As can be seen in Figure 4.9(b), the progress in the oxidation, especially the increment of Fe^{2+}(II) in oxides, in all samples was noticed after aging time of 40 days. However, the different in the initial wettability could not be explained with the result in that there is little difference between the spectra. Therefore, it needs to implement additional surface analysis to fully account for the difference in the initial wettability depending on the additional heat treating.

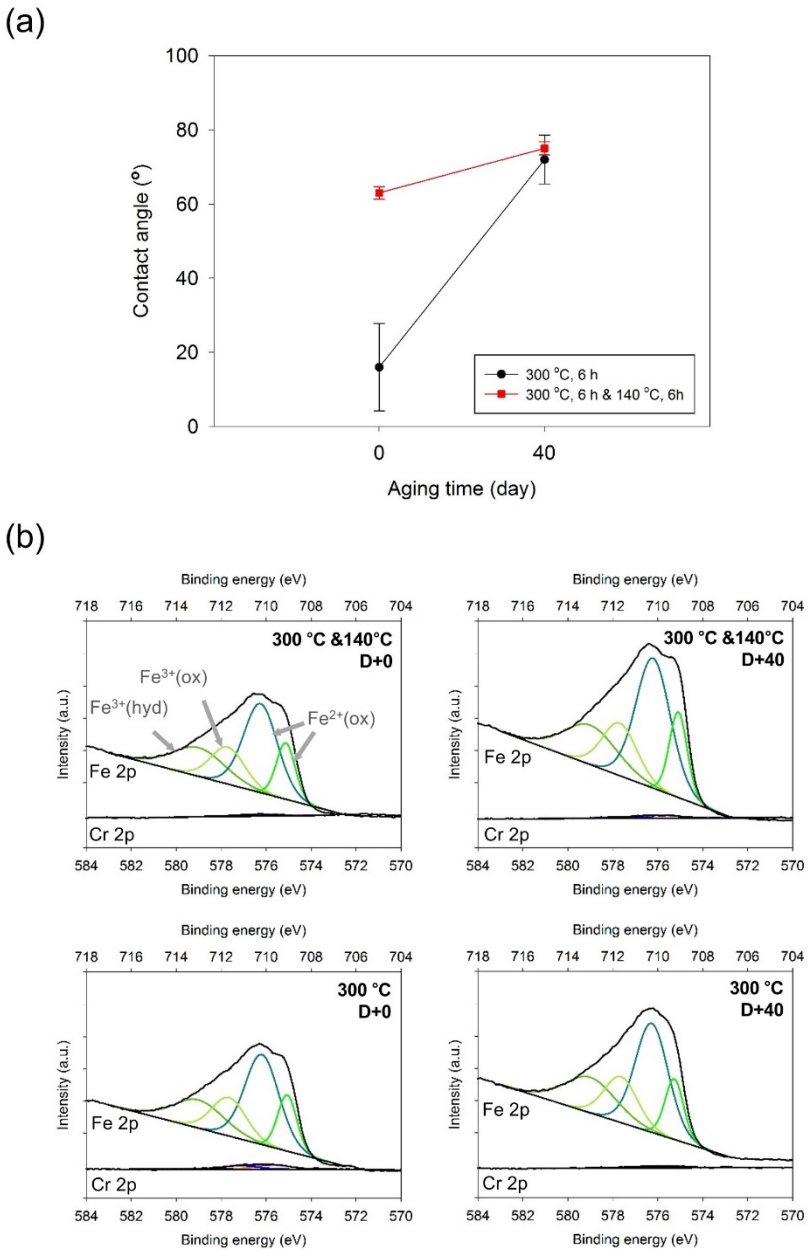

Figure 4.9 (a) Change in CA by additional heat treating for aging time of 40 days (b) XPS spectra of Fe 2p and Cr 2p depending on heat treating conditions and aging time.

4.5 Influence of phase transformation

It is found to be difficult to directly relate the wettability with the phase structure of the surface layer. Figure 4.10 (a) ~ (c) shows XRD(X-ray diffraction) patterns of stainless steel surfaces prepared with different heat treating conditions. XRD analysis is an effective analytic method used to study the phase structure of a material. Results visualize that there mainly exist γ-phase(austenite) at the surface layer as well as a slight amount of α'-phase(martensite) in all samples. A small amount of martensite is thought to be generated in the mechanical grinding and polishing, as can be seen in Figure 4.10(d).[61] Resultant wettability of the samples was found to be different depending on heat treating condition. Therefore, it can be concluded that there was little relationship between the wettability and the phase composition of the outermost surface layer.

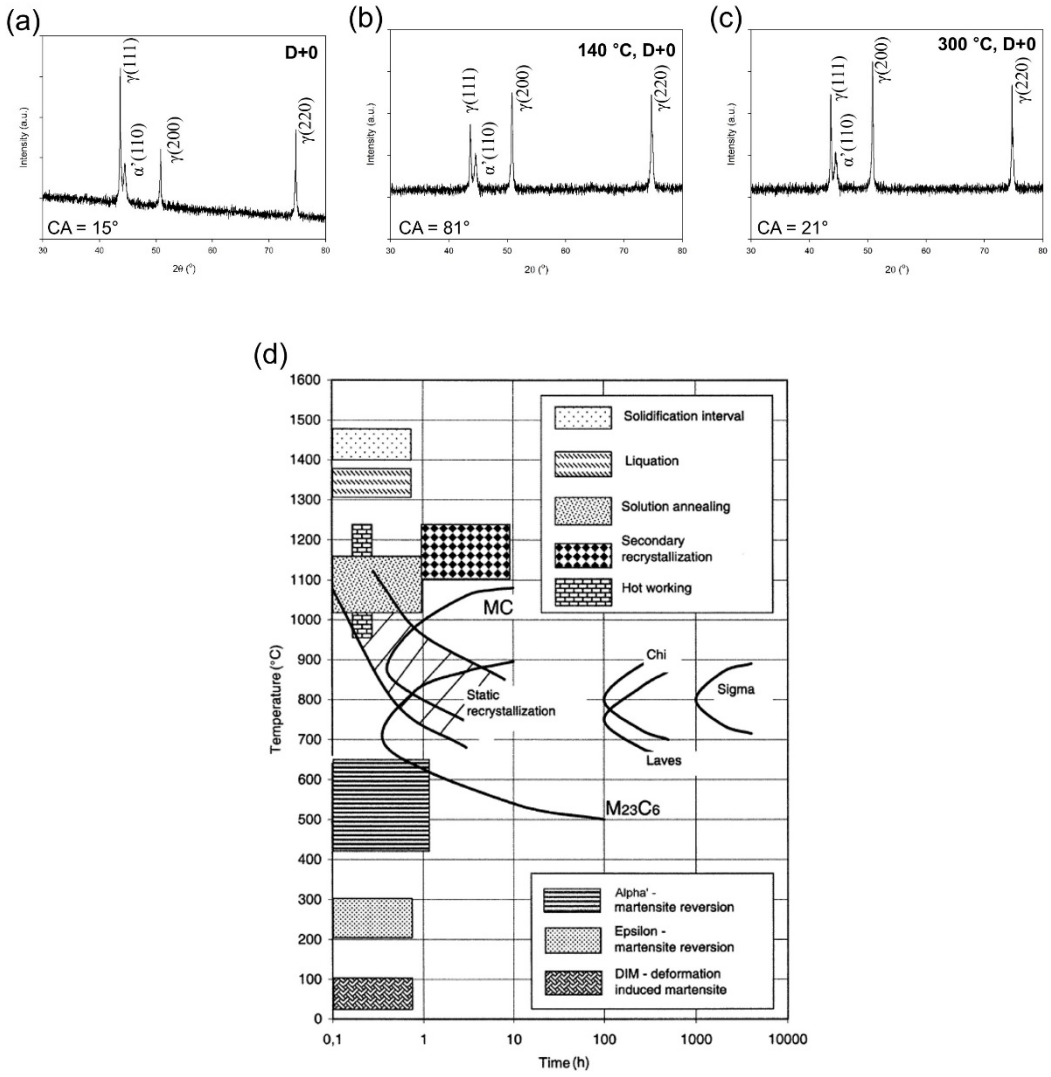

Figure 4.10 XRD patterns of (a) polished sample and heat-treated samples at (b) 140 °C and (c) 300 °C for 6 h showing the existence of γ-phase(austenite) as well as α'-phase(martensite). (d) Phase transformations in austenitic stainless steels depending on heat treating time and temperature.[61]

4.6 Electrical property of heat-treated surfaces

Th electrical property of heat-treated STS surfaces was characterized to have a low sheet resistance suitable for various applications such as PEMFC (proton-exchange membrane fuel cell).[62-63] Table 4.2 presents the result of measuring sheet resistance using PPMS (physical property measurement system, PPMS-14, Quantum Design, USA). Six samples were prepared as described in the table to verify the influence of heat treating to the electrical property. Four electrical probes were positioned in-line to calculate four-point sheet resistance.[64] During the measurement, temperature was set to be 298 K. Measurement was repeated 10 times so that data could be presented as average and standard deviation. Sheet resistance of the samples was derived to be in the range from 0.46 to 1.04 mΩ/sq, which supports the potential feasibility of the material to be utilized for components of energy devices such as bipolar plates of fuel cells.

Table 4.2 Sheet resistance of heat-treated STS 304 samples

Sample number	Description	Sheet resistance (mΩ/sq)
1	Polished, day 0	0.54±0.03
2	Polished, day 75	0.46±0.13
3	Heat-treated at 140°C, day 0	1.04±0.13
4	Heat-treated at 140°C, day 75	0.91±0.03
5	Heat-treated at 300°C, day 0	0.41±0.09
6	Heat-treated at 300°C, day 75	0.56±0.31
Reference[65]	Stainless steel 304	0.4764

5. Demonstration of fabricating superhydrophobic and superhydrophilic stainless steel surface

Superhydrophobic or superhydrophilic surfaces now can be achievable without difficulty in a laboratory scale, by following the biomimetic design rule which was established by studying diverse natural surfaces with marvelous wettability such as lotus leaves. The key concept nature tells us for wettability control is that macroscopic wettability is determined by the microscopic structures on the surface as well as the intrinsic wettability of biological materials. However, beyond the boundary of the laboratory, achieving robust and durable superhydrophobic and superhydrophilic surfaces is extremely challenging due to harsh, accidental and unpredictable external stimulus which can deteriorate wettability.

Engineering metals such as iron, aluminum, copper and their alloys are expected to be a powerful candidate to fabricate durable superhydrophobic and superhydrophilic surfaces due to the wide applicability of the materials to the frontline of industry. Fabrication technology in micro- and nanoscale has been developed and this leads to development of wettability control technology by

structuring the surface. Nowadays machining metallic materials in microscale is achievable due to significant advance in various micromachining processes including non-traditional machining methods such as electrical discharge machining (EDM), laser beam machining (LBM), or electrochemical machining (ECM), enabling wettability control of engineering metal surfaces.

Most of previous research is limited in two aspects: 1) time-consuming fabrication of superhydrophobic surfaces, and 2) difficulty in achieving superhydrophilic surfaces. Realizing superhydrophobic surfaces inevitably involves aging effect on the wettability. This was observed in previous research, yet the solution to shorten the aging time has been little handled as an important issue so far, rather, aging effect has been regarded insignificantly and even neglected. Recent reports pointed out such problems and suggested a solution by heat treating at a specific temperature, yet the solution is still limited in that temperature effect was not investigated. In addition, there are few reports of superhydrophilic metal surface, especially made with stainless steel. The problems have been dealt with by chemical coatings after structuring the surface of metals, which is also limited in the view of robustness and durability.

In this chapter, fabrication of superhydrophobic and superhydrophilic stainless steel surfaces is demonstrated in consideration of aging effect. To tackles existing problems raised above, heat treating and micromachining methods are

exploited. This approach provides answers to the two problems raised above: 1) the feasibility rapid fabricating superhydrophobic surface 2) superhydrophilic stainless steel surface without chemical coatings.

5.1 Experimental setup

Figure 5.1 describes the experimental setup for fabricating superhydrophobic and superhydrophilic stainless surfaces. The fabrication process is composed of laser beam machining, electrochemical etching, and heat treating in serial order.

Figure 5.2 shows the system of nanosecond-pulsed laser beam machining. Laser beam machining was conducted to groove the surface of stainless steel (type 304, Nilaco Co., Japan) samples cut in the size of $15 \times 15 \times 1$ mm^3. A more detail specification of the system is presented in Table 5.1. The general size of grooves was in tens of millimeters and the geometry was controlled to change the machining parameter, as previously demonstrated by S. W. Lee et al.[66]

The recast layer generated on the machined surface was removed by electrochemical etching, referring to experimental setup of H. S. Shin et al.[67] Etching parameter is presented in Table 5.2. Sonicating the etched samples in deionized water thoroughly cleaned the residual debris from the surface.

Heat treating was performed on the structured and etched samples. Samples were dried in blown air stream and stored in a furnace for 6 hours. In case of fabricating superhydrophobic surface, heat treating temperature was set at 140 °C to instantaneously realize the designed wettability by shortening aging time. In case

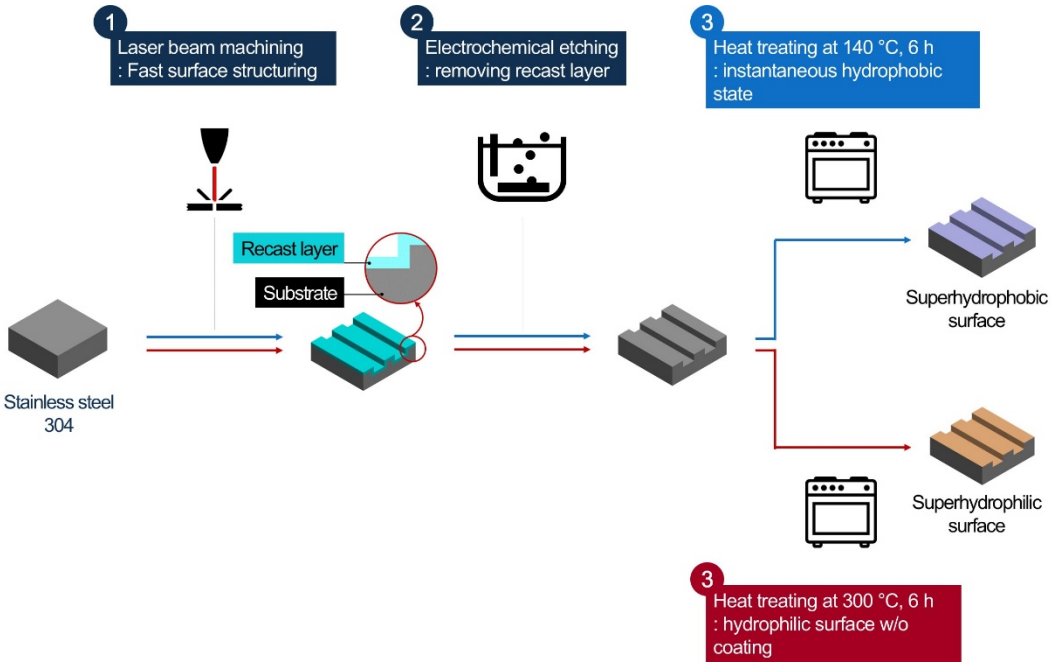

Figure 5.1 Schematic illustration of fabrication superhydrophobic and superhydrophilic stainless steel surfaces.

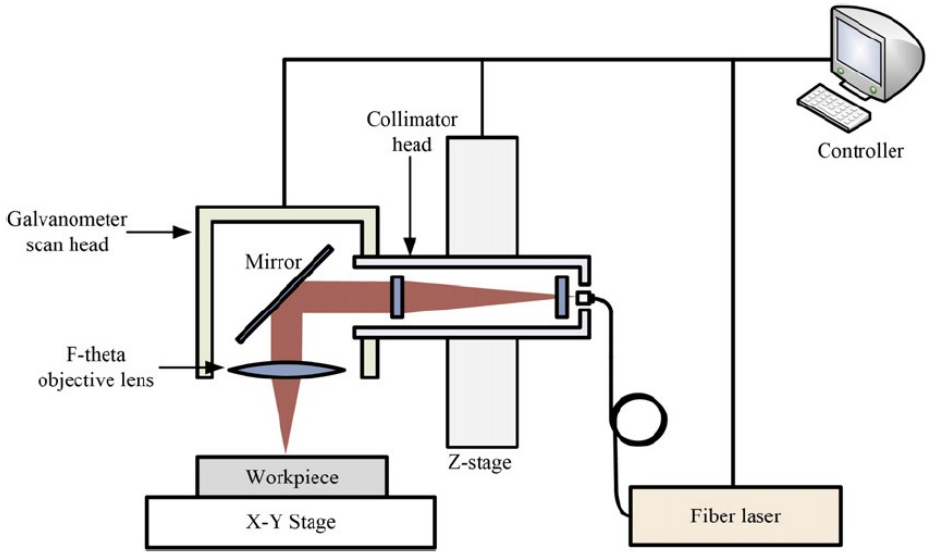

Figure 5.2 Schematic illustration of the system of laser beam machining[66]

Table 5.1 Specification of the laser beam machining system.

Type	Yb-doped pulsed fiber laser
Workpiece	Stainless steel (type 304)
Wavelength	1064 nm
Scan speed	258.6 mm/s
Repetition rate of pulsed laser	20 kHz
Pulse length	100 ns
Power	10 W

Table 5.2 Specification of the electrochemical etching[67-68]

Working electrode (anode)	Stainless steel (type 304)
Counter electrode (cathode)	Platinum
Electrolyte	$NaNO_3$
Concentration	1 M
Applied voltage	15 V
Etching time	600 s

of fabrication superhydrophilic surface, temperature was set at 300 °C to modify the surface of stainless steel to be hydrophilic.

5.2 Surface structuring by laser beam machining

To realize superhydrophobic or superhydrophilic surfaces, microgrooves were fabricated by using laser beam machining. Laser beam machining is one of fastest and easiest non-contact machining methods for structuring the surface of metals in microscale. In order to groove the surface, laser beam path was prepared as a group of repetitive lines covering the target surface.

Microgrooves with different size of groove width and groove depth were fabricated by controlling machining and laser beam path parameters. Because laser beam machining is based on thermal energy to remove materials from the bulk, machined geometry can be affected not only by laser beam path, but also by various parameters such as input power, scan speed, number of scan. Here, the machining parameters of input power, scanning speed were fixed at 10 W and 258.6 mm/s, and the laser beam path parameters of pitch and line interval were set at 50 μm and 20 μm, respectively. As presented in Table 5.3, various microgrooves with different groove width and groove depth were fabricated by changing parameters as follows: number of scan by 5, 10, 15 times and number of line by 1, 2.

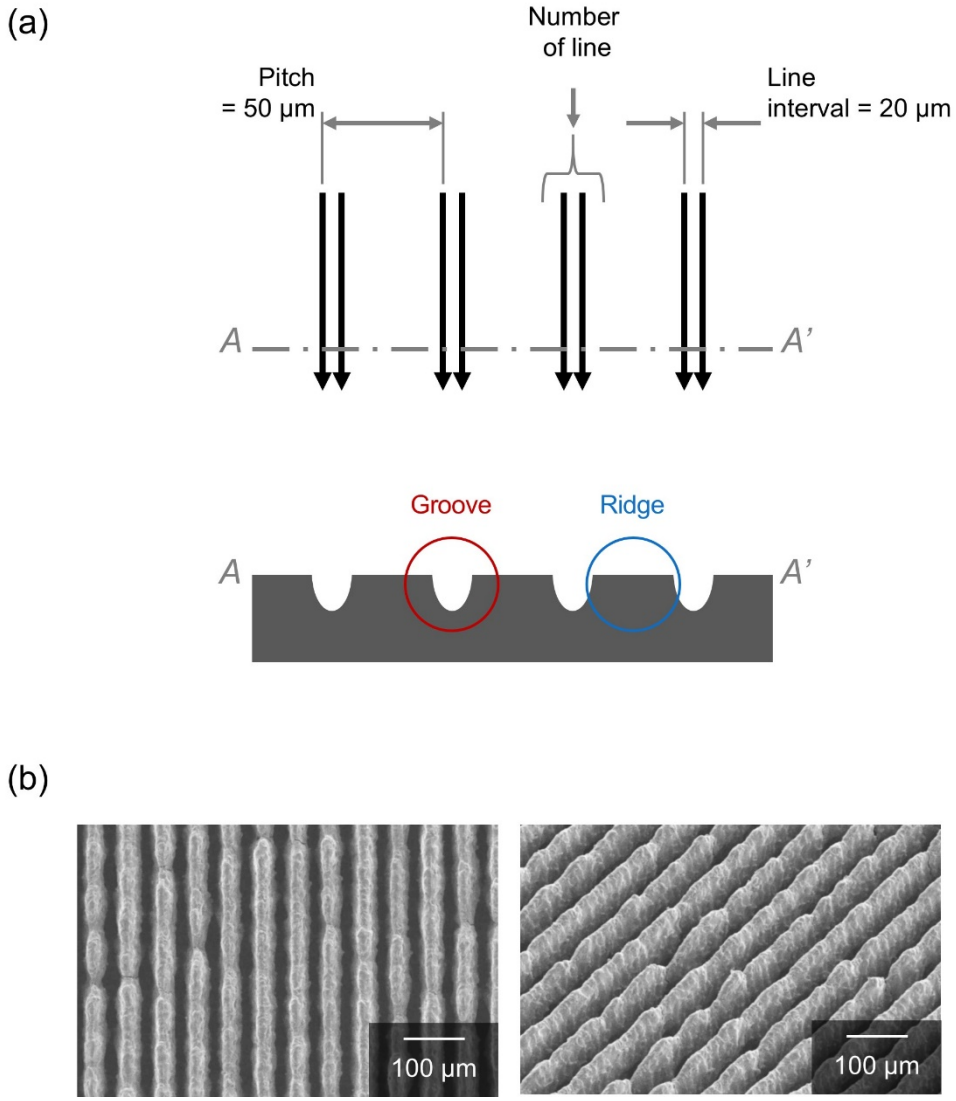

Figure 5.3 (a) Schematic illustration of machining parameters to control the geometry of grooves by laser beam machining. (b) Representative SEM images of microgroove (number of line = 1, number of scan = 15)

Recast layer was observed on the surface of microgrooves, which was to be removed before heat treating. Nanosecond-pulsed laser beam generates recast layer after machining. Recast layer is the portion of resolidified material which was melted by laser beam but failed to be ejected from the cavity. The chemical composition of recast layer is mainly metal oxides, which can be different from the surface of original metal before laser beam machining. Therefore, the recast layer was needed to be removed so that the unaffected surface under recast layer could be exposed for heat-treating.

Table 5.3. Structure geometry of fabricated microgrooves.

Parameters		Fabricated microgrooves	
Number of line	Number of scan	Groove width (μm)	Groove depth (μm)
1	5	39	23
	10	40	46
	15	38	110
2	5	60	29
	10	60	99
	15	60	154

5.3 Removal of recast layer by electrochemical etching

Electrochemical etching successfully removed the recast layer generated on the top of the machined surfaces by laser beam machining. Electrochemical etching is an effective micromachining method to remove the materials on the surface with a large area.[13] Combined with laser beam machining for rough structuring, electrochemical etching can be utilized as an effective finishing method to remove recast layer, improving the fidelity of structures. [69-70] Figure 5.4 shows the change of microgrooves (number of line = 1, number of scan = 20) before and after etching. The topographical feature of recast layer, melted and resolidified portion on the structure could be found on the surface of grooves before etching. After etching, the feature was hardly found on the structure. Energy-dispersive spectroscopy was conducted to confirm the removal of recast layer. Two samples were prepared by grooving both samples with laser beam machining and one of the two samples was etched selectively. As shown in Table 5.4, difference in the amount of oxygen was detected by comparing two samples. As the recast layer consists of complex oxides, smaller amount of oxygen in the etched sample suggests that recast layer on the surface was successfully removed.

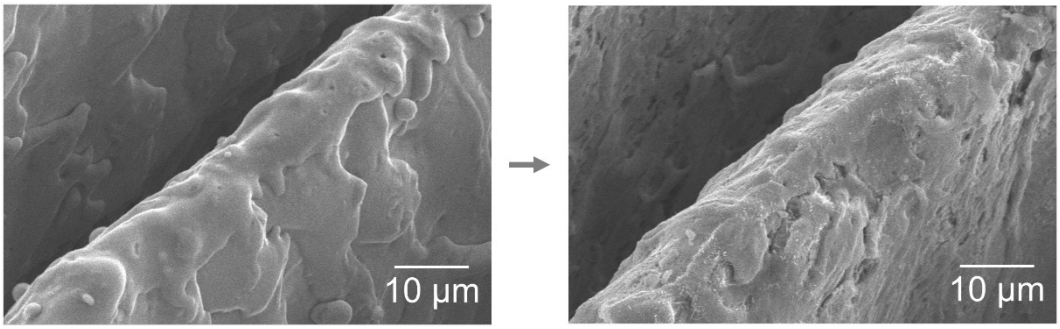

Figure 5.4. SEM images of recast layer on the structure and the structure without recast layer.

Table 5.4 Weight percent comparison of elements by EDS analysis.

	Laser beam machining	Laser beam machining and electrochemical etching
Fe, Cr, Ni	82.2	90.9
O	17.8	9.1

Removing recast layer was critical to restore the surface and to activate the heat treating effect on the surface of microgrooves. Figure 5.5 exhibits the effect of electrochemical etching for heat treating (300 °C, 6 h) to achieve hydrophilic surfaces. Laser beam machining (number of line = 1, number of scan = 5) was performed on two stainless steel samples for surface structuring. Sample shown in Figure 5.5(a) was etched and heat-treated at 300 °C for 6 h. The other sample shown in Figure 5.5(b) was heat-treated at 300 °C for 6h directly after laser beam machining. Both samples demonstrated superhydrophilic property when 5 μl of deionized water droplet was lied on each surface. The samples were stored in ambient air for 5 days and wettability was characterized again in the same manner. While the sample shown in Figure 5.5(a) holds superhydrophilic property, the sample shown in Figure 5.5(b) lost initial superhydrophilic property. In can be inferred that heat treating for hydrophilic surfaces was selectively effective on the sample with the etched surface, which is analogous to the freshly polished stainless steel surface in chemical perspective. Heat treating on the other surface was not effective due to the recast layer which possesses different chemical composition from the freshly polished stainless steel, being inactive to heat treating.

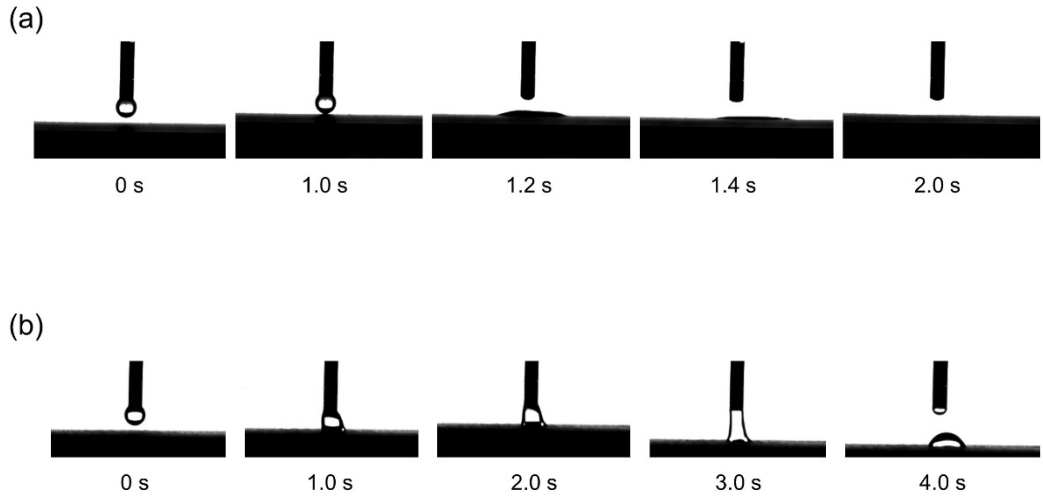

Figure 5.5. Snapshots of water droplet lying on the superhydrophilic surface after 5 days from the fabrication process, showing the effect of electrochemical etching for heat treating. Machining conditions are as follows: (a) laser beam machining, electrochemical etching and heat treating (300 °C, 6 h) in serial order (b) laser beam machining and heat treating at the same condition.

5.4. Superhydrophobic stainless steel surfaces

Fabrication of superhydrophobic stainless steel surfaces was demonstrated by laser beam machining, electrochemical etching and exploiting heat treating (140 °C, 6 h) to shorten aging time. Figure 5.6(a) displays the photograph of the fabricated sample. To structuring the surface of stainless steel, laser beam path parameters was selected as follows: number of line = 1 and number of scan = 5. This is to realize microgrooves with as minimum size as possible while the structural fidelity is not compromised using the laser beam machining system. Laser beam machining yielded surface-structured stainless steel with minimal microgrooves (groove width = 39 μm, ridge width = 11 μm, and groove depth = 23 μm), followed by electrochemical etching. Heat treating at 140 °C for 6 h was applied to the etched sample consecutively to finish the superhydrophobic stainless steel surface. Figure 5.6(b) displays the SEM image of the fabricated sample showing a regular pattern of microgrooves on the surface. Inset image is the surface of a ridge, showing that recast layer was successfully removed by electrochemical etching. The fabricated sample exhibited extreme water-repellency as shown in Figure 5.6(c).

Wettability of the fabricated sample was characterized to have CA of 151° and explained in Cassie-Baxter model. CA was measured before and after

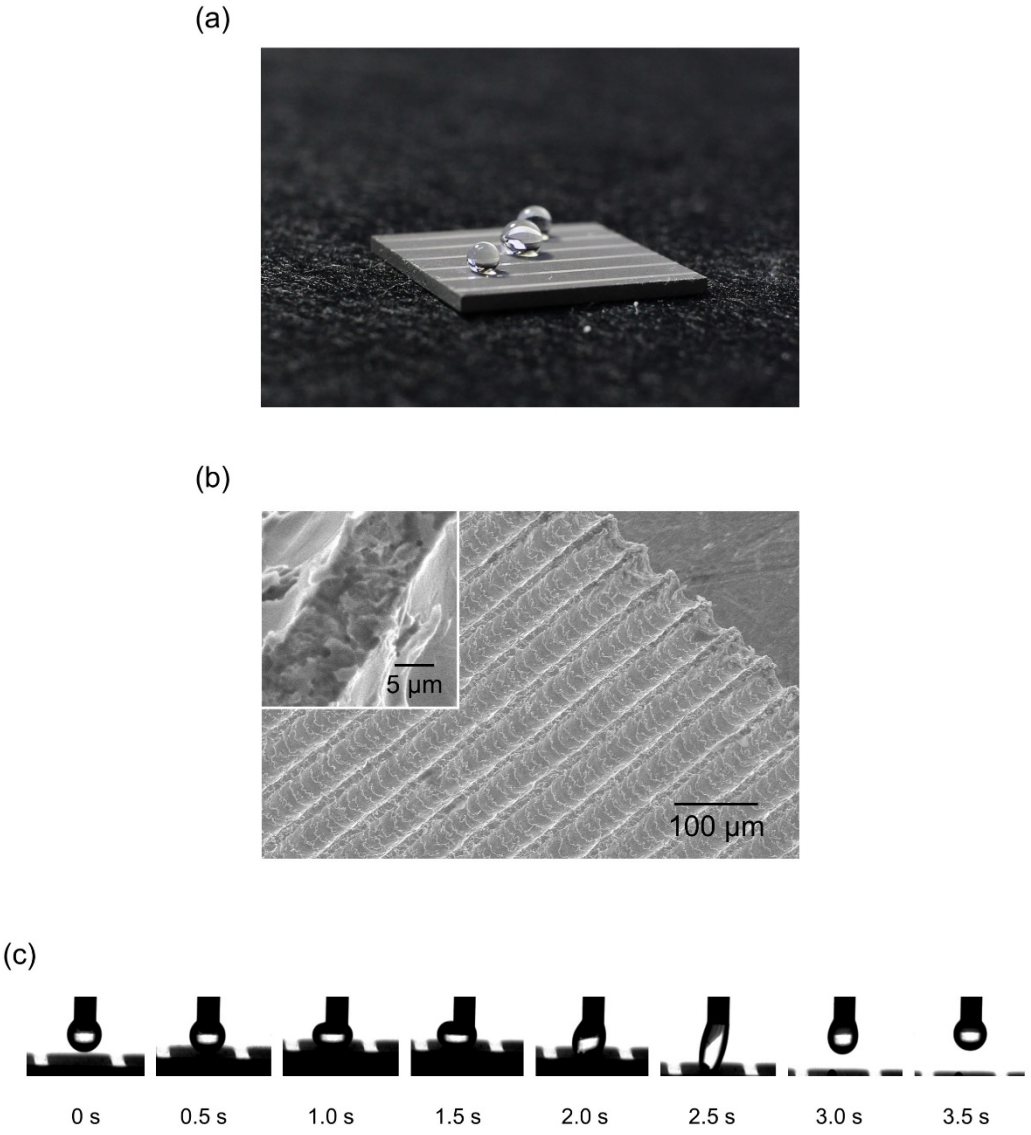

Figure 5.6 (a) Photograph of superhydrophobic stainless steel surface exhibiting superhydrophobic property. (b) SEM image of the fabricated sample. Inset shows the surface of a ridge without recast layer. (c) Snapshots of a water droplet squeezed between the dispensing needle and the surface.

heat treating and the result is presented in Figure 5.7(a). As soon as electrochemical etching was done, the surface was hydrophilic. This can be compared to the wettability of the freshly polished stainless steel, as demonstrated in Chapter 3. Laser beam machining added the roughness effect on the wettability,[34] resulting in superhydrophilic surface with unmeasurable CA (CA = 0°). After heat treating at 140 °C for 6 h, which is for achieving hydrophobic surfaces, the sample readily exhibited superhydrophobic property. This corresponds to the heat treating effect of shortening aging time, explained in Chapter 4. To further explain the resultant wettability, theoretical value of Cassie-Baxter and Wenzel model, as explained in Chapter 2, could be calculated to compare the measured CA as:

$$\cos\theta^{*} = r\cos\theta \qquad \text{(Wenzel)}$$

$$\cos\theta^{*} = rf_{s}\cos\theta + f_{s} - 1 \qquad \text{(Cassie-Baxter)}$$

where roughness factor (r) and fraction of liquid/solid interface (f_s) are calculated to be r = 2.1, f_s = 0.2, respectively, following the geometry of the fabricated sample. Figure 5.7(b) presents the comparison between theoretical value of the two models and measured CA on the superhydrophobic surface. The *x*-axis error bar of the measured CA stands for the minimum and maximum value of chemical angle just after heat treating at 140 °C, which was obtained in Chapter 4. Measured CA on the superhydrophobic surface tends to overlap on the theoretical value of Cassie-Baxter model, proposing that the water droplet lies on the mixture of solid and air, without

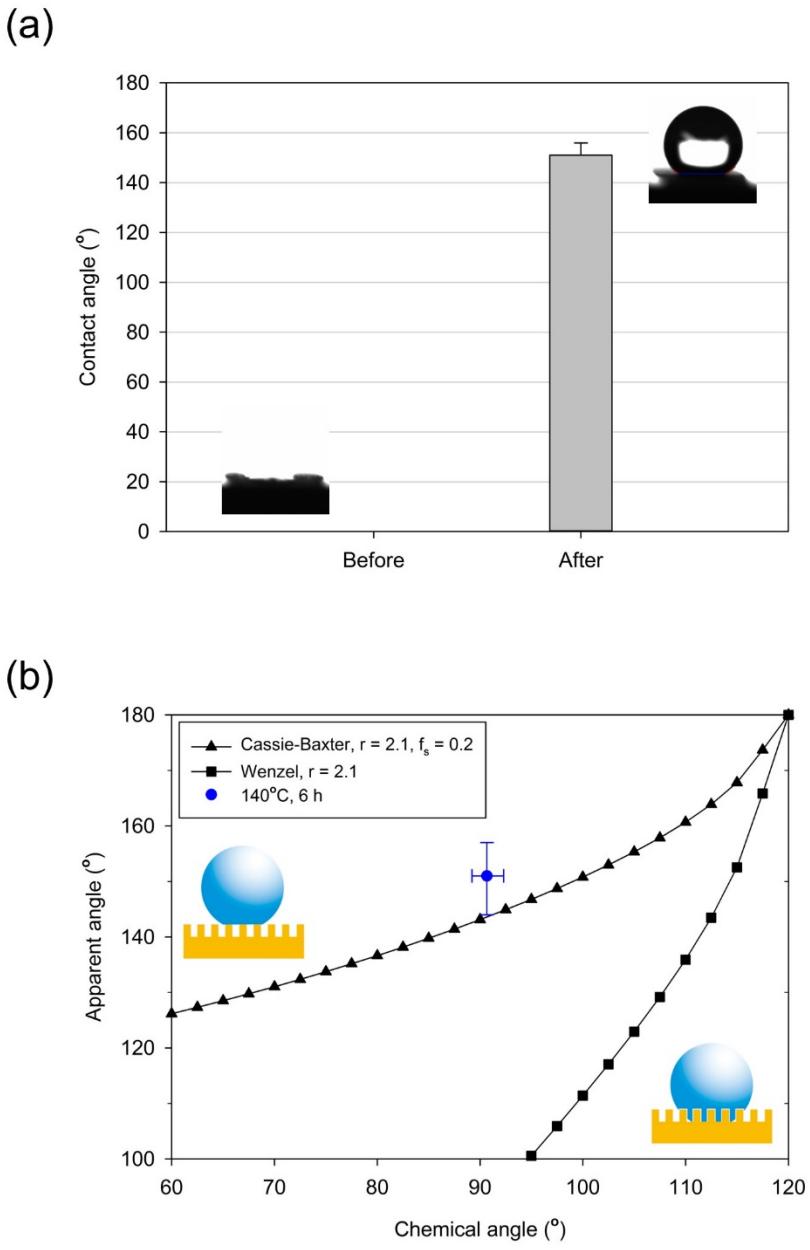

Figure 5.7 (a) Change in CA before and after heat treating at 140 °C for 6 h. (b) Resultant wettability of the superhydrophobic surface corresponded to Cassie-Baxter model.

intruding inside the microgrooves on the surface.

5.5 Superhydrophilic stainless steel surfaces

Fabrication of superhydrophilic stainless steel surface was demonstrated in consideration of aging effect, which guarantee long-lasting wettability. The fabrication process of superhydrophilic surfaces is identical to that of superhydrophobic surfaces, except that the heat treating temperature was set to 300 °C to modify the wettability for intrinsic hydrophilic surface. To induce superhydrophilic property on the surface, microgrooves with high aspect ratio is needed to maximize the roughness effect on the wettability.[34] Therefore, machining parameters and laser beam path parameters were further expanded.

Groove aspect ratio was verified to be critical to hold superhydrophilic property as time passes. Table 5.5 presents the results of sample fabrication for achieving superhydrophilic stainless steel surfaces and representative image can be found in Figure 5.8(a). Figure 5.9 shows the change in CA after 40 days of aging time. While superhydrophilic property was observed at the sample with groove aspect ratio larger than 2.4, loss of superhydrophilic property was also observed at samples whose groove aspect ratio is lower than 2.2 after 40 days of fabrication process. It can be concluded that the minimum value of groove aspect ratio is 2.4 in order to realize superhydrophobic surfaces with the fabrication process.

Table 5.5 Surface geometry and resultant wettability of the fabricated samples for superhydrophilic property.

Parameters		Surface geometry			Surface characterization	
Number of line	Number of scan	Groove width (μm)	Groove depth (μm)	Groove aspect ratio	CA after fabrication (°)	CA after 40 days (°)
1	5	39	23	1.2	0	50
	10	40	46	2.2	0	13
	15	38	110	6.1	0	0
2	5	60	29	0.7	0	68
	10	60	99	2.4	0	0
	15	60	154	3.8	0	0

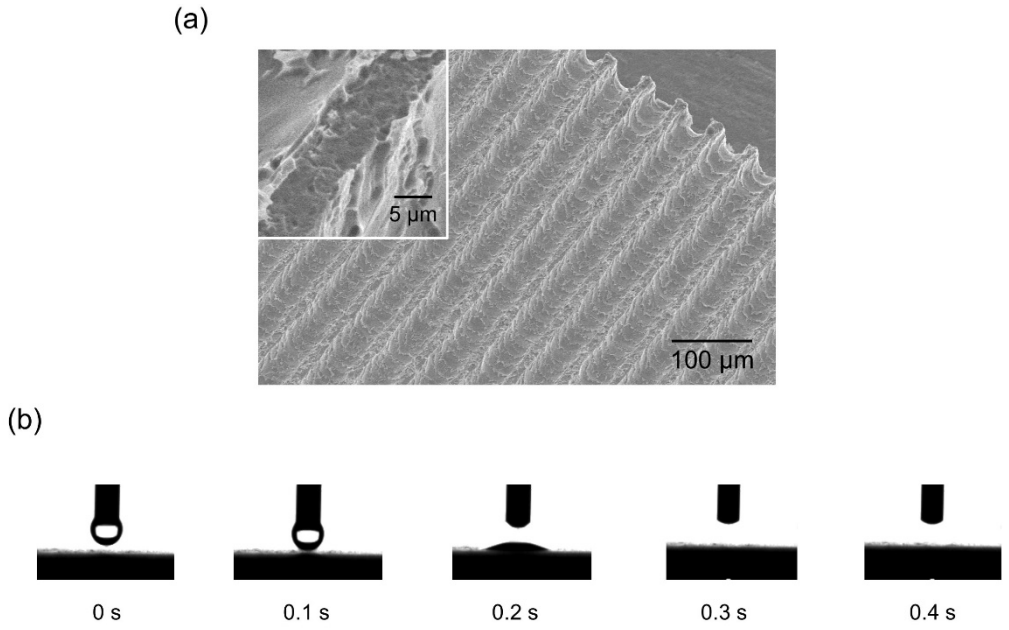

Figure 5.8 (a) Representative SEM image of fabricated samples for superhydrophilic surfaces (number of line = 1, number of scan = 10). Inset image displays successful removal of recast layer by electrochemical etching on the surface. (b) Snapshots on the spontaneous wetting of water droplet on the sample (number of line = 2, number of scan = 15) after 40 days from the fabrication process.

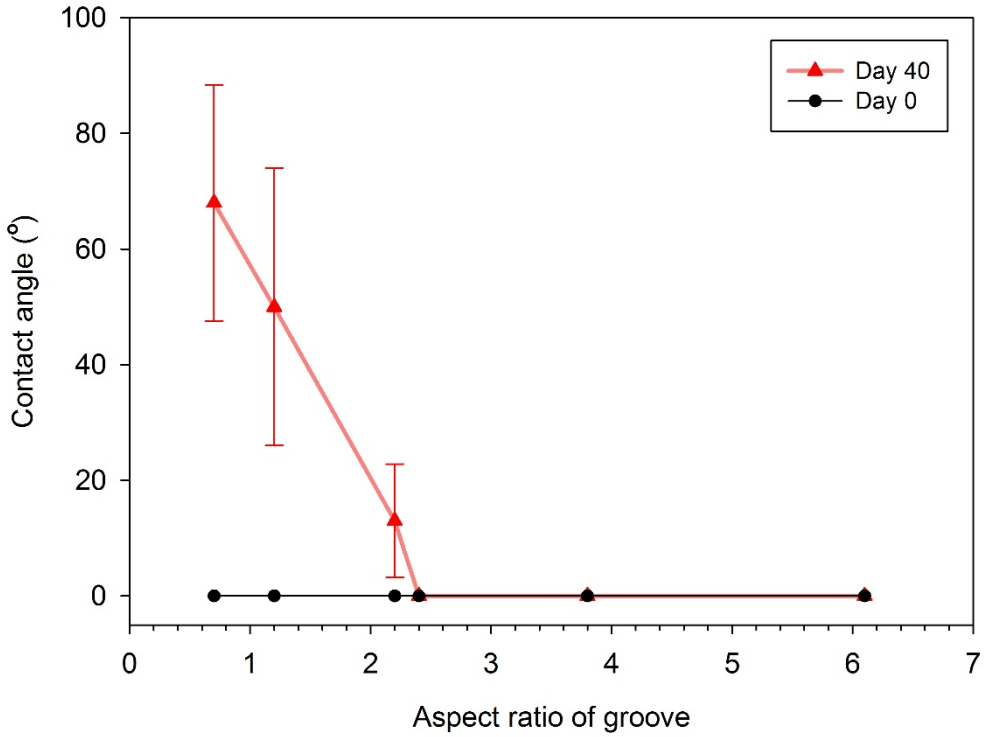

Figure 5.9 Change in CA depending on the aspect ratio of the grooves after 40 days of aging time.

To elaborate on the relationship between groove aspect ratio and the resultant wettability of the samples after 40 days of aging time, a simple model is applied here for the liquid progression in a rectangular groove as displayed in Figure 5.10(a).[34, 71] Assuming that the menisci of the liquid in the groove and gravity effect can be ignored, surface energy change *dE* in the liquid progression can be expressed as following:

$$dE = (\gamma_{SL} - \gamma_{SA})(2d + w)dx + \gamma w dx \quad (1)$$

where γ_{SL}, γ_{SA}, and γ refer to surface energy of solid/liquid, solid/air and liquid/air., respectively. Substituting equation (1) by Young's equation, *dE* is expressed in terms of the groove geometry as:

$$dE = \gamma\left(w - (2d + w)\cos\theta\right)dx \quad (2)$$

where θ refers to chemical angle of the solid. The theoretical boundary of liquid progression explicitly derived from (2) by letting *dE* = 0, which leads to the expression as:

$$\theta_c = \arccos\left(\frac{1}{2(d/w)+1}\right) \quad (3)$$

which suggests the relationship of groove aspect ratio (*d/w*) with chemical angle of the solid θ_c. In other words, θ_c stands for a geometric criteria determining whether liquid progression is favorable or not. Therefore, in case liquid progression is favorable (*dE* < 0), the condition of $\theta < \theta_c$ must be satisfied.

Figure 5.10(b) first suggests the importance of groove aspect ratio for

(a)

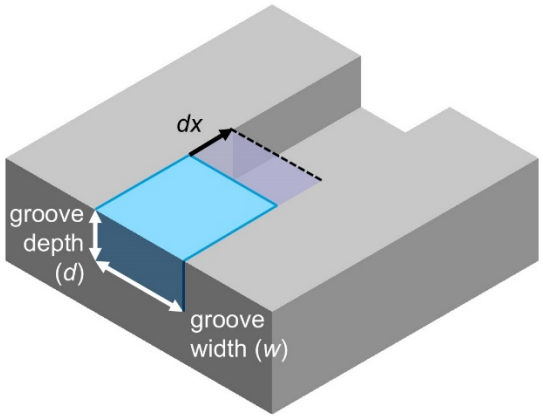

(b)

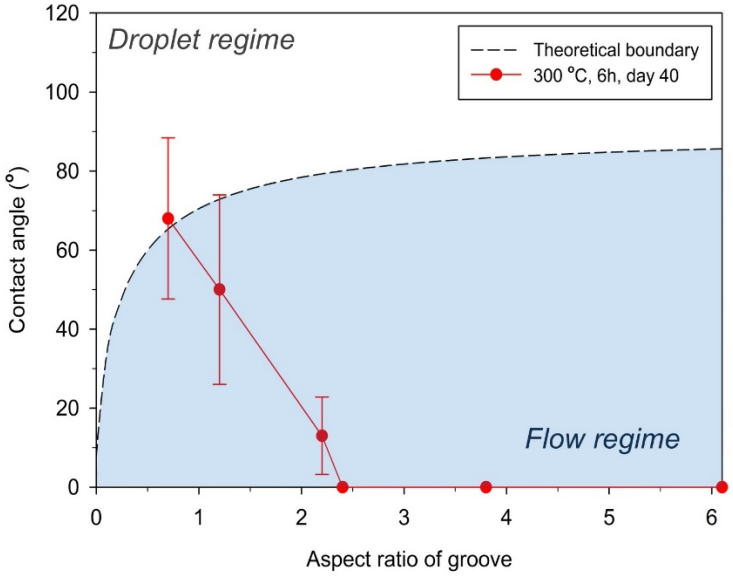

Figure 5.10 (a) Schematic illustration of the liquid progression (*dx*) in a groove. (b) Plot explaining the influence of groove aspect ratio and chemical angle on superhydrophilic surfaces.

fabricating superhydrophilic surfaces with microgrooves on the surface. As groove aspect ratio become larger, liquid is more likely to flow in a groove, resulting in a superhydrophilic surface. Chemical angle for $dE < 0$ increases as groove aspect ratio increases. In case of $d/w = 1.0$, $\theta < 70.5°$ should be satisfied for spontaneous wetting. In case of $d/w = 2.0$, however, $\theta < 78.5°$ should be satisfied. This can be interpreted that higher groove aspect ratio is required to achieve superhydrophilic surfaces with a more hydrophobic material.

In addition, Figure 5.10(b) explains the reason for the loss of superhydrophilic property in the d/w range from 0.7 to 2.2. Lost superhydrophilic property was attributed to aging effect; as time passes, surface of material (chemical factor) become more hydrophobic, leading to increase in chemical angle. When aging effect is fully expressed on the wettability, chemical angle rises up to ~80°. In this case, the condition of $\theta < \theta_c$ is not satisfied anymore, which eventually results in the loss of superhydrophilic property. Measured CA data corresponds to the explanation above in that samples with groove aspect ratio of 2.4 to higher held superhydrophilic property after 40 days from fabrication process. At the groove aspect ratio of 2.4, θ_c is 80.1, which is slightly lower than the maximum of observed CA from heat treating at 300 °C, for 6 h, as presented in Chapter 4.

6. Conclusion

The influence of aging and heat treating on the wettability of stainless steel is investigated, which demonstrates a technical breakthrough in an increasing demand for superhydrophobic and superhydrophilic metal surfaces. Aging effect is a major obstacle to the wettability control of metal surfaces which results in time-consuming fabrication process for superhydrophobic surfaces and difficulty in achieving superhydrophilic surfaces. Aging effect is demonstrated and the explanation is provided on the influence of oxygen from which heat treating is deduced as an effective solution to handle the issue of aging effect. By demonstrating the fabrication of superhydrophobic and superhydrophilic stainless steel surfaces, it is verified that considering aging and heat treating effects in the fabrication process is critical to overcome the obstacle of low throughput and limited potential of the wettability control technology for engineering metals.

Aging effect on the wettability of STS surface is investigated and it was explained that oxygen in the environment is one of the dominant factors behind the phenomenon. Samples of STS 304 were mechanically ground and polished to

control the surface roughness that highly affects the apparent wettability. We monitored CAs of 5 μl water droplet on the polished STS 304 samples daily and we observed a significant increase in the CAs in the first three days from the initial state. To identify the role of oxygen and moisture in the aging effect, four samples were prepared and respectively stored in a controlled environment where the amount of oxygen and water was regulated for 5 days. After measuring CAs on the stored samples, a correlation was found between oxygen and the wettability, while an effect of water was not detected. XPS analysis was conducted to further study the influence of oxygen and the relationship between transitional oxidation state and aging effect was suggested. Additionally, the aging effect on the surface-structured STS surface was demonstrated, which proposes usefulness of STS for superhydrophobic surfaces not requiring post-treatment. Exploiting aging effect would be beneficial to understanding the wetting behavior of various wettability-controlled metallic surfaces and broaden the material potential of STS for durable, robust and practical functionalized surfaces.

Heat treating effects on the wettability of stainless steel was investigated and it was verified that it works to shorten aging time and to realize hydrophilic stainless steel surface. Temperature range from 50 °C to 400 °C and time range from 1 h and 48 hours were explored and the resultant wettability by heat treating was quantified by measuring CA of water. After heat treated at 140 °C for 6 h, the

surface of a polished stainless steel sample readily exhibited increase CA of 91° which had shown CA of ~20° before heat treating. The wettability lasts over 200 days holding hydrophobic property with final CA of ~95°. Heat-treated samples at 300 °C for 6 h showed lasting hydrophilic state even after about 200 days, which suggest the possibility of intrinsic wettability change by heat treating.

Fabrication of superhydrophobic and superhydrophilic stainless steel surfaces is demonstrated in consideration of aging and heat treating effect. Laser beam machining, electrochemical etching, and heat treating was performed on stainless steel samples (type 304) consecutively. For superhydrophobic surface, heat treating condition was set at 140°C for 6 h. For superhydrophilic surface, heat treating temperature of 300 °C was selected. Fabricated superhydrophobic and superhydrophilic surfaces were characterized by measuring CA. Explanations on the resultant wettability were given based on Cassie-Baxter model and a simple liquid progression model, respectively.

Technical improvement and academic contribution of this dissertation is summarized Table 6.1 While advanced materials attracts a lot of attention due to excellent material properties, still, the industry of today heavily relies on engineering metals with broad applications in the whole realm of the industry. It is practically difficult to find alternative materials to replace because of the superior material properties and economics feasibility. It is highly expected that controlling

wettability of engineering metals even extend the applications of engineering metals with enhanced functionality, which will lead to creating new value and market opportunities. To this end, it is necessary to achieve industry-friendly fabrication technology for controlling the wettability of engineering metals. This dissertation provides guidelines for aging effect which is inevitable in the fabrication process, and for dealing with it by utilizing heat treating effect.

Table 6.1 Summarized conclusion of the dissertation.

Topic	Previous issue	Improvement	Contribution
Aging effect	Observing on structured surface	Observing on flat surface	Providing information on chemical angle
	Controversial explanation	Explaining influence of oxygen	Deducing heat treating as solution for aging effect
Heat treating effect	Shortening aging time at a specific temperature on structured surface	Suggesting heat treating temperature by examining various conditions on flat surface	Investigating heat treating temperature effect on the wettability of stainless steel
	Little investigation on hydrophilic state	Realizing hydrophilic stainless steel surface	Extending the domain of the technology to hydrophilic surface
Superhydrophobic metal surface	Time-consuming fabrication to realize superhydrophobic surface	Achieving superhydrophobic surface in 6 h by heat treating	Improving commercial potential of the technology
Superhydrophilic metal surface	Difficulty in realizing superhydrophilic surface	Achieving long-lasting superhydrophilic surface	Improving commercial potential of the technology

References

[1] Sun, T.; Feng, L.; Gao, X.; Jiang, L., Bioinspired surfaces with special wettability. *Accounts of chemical research* **2005,** *38* (8), 644-652.

[2] Darmanin, T.; Guittard, F., Superhydrophobic and superoleophobic properties in nature. *Materials Today* **2015,** *18* (5), 273-285.

[3] Solga, A.; Cerman, Z.; Striffler, B. F.; Spaeth, M.; Barthlott, W., The dream of staying clean: Lotus and biomimetic surfaces. *Bioinspiration & biomimetics* **2007,** *2* (4), S126.

[4] Sun, Z.; Liao, T.; Liu, K.; Jiang, L.; Kim, J. H.; Dou, S. X., Fly-Eye Inspired Superhydrophobic Anti-Fogging Inorganic Nanostructures. *Small* **2014,** *10* (15), 3001-3006.

[5] Wong, T.-S.; Sun, T.; Feng, L.; Aizenberg, J., Interfacial materials with special wettability. *Mrs Bulletin* **2013,** *38* (5), 366-371.

[6] Bico, J.; Tordeux, C.; Quéré, D., Rough wetting. *EPL (Europhysics Letters)* **2001,** *55* (2), 214.

[7] Liu, K.; Jiang, L., Metallic surfaces with special wettability. *Nanoscale* **2011,** *3* (3), 825-838.

[8] Chu, W.-S.; Kim, C.-S.; Lee, H.-T.; Choi, J.-O.; Park, J.-I.; Song, J.-H.; Jang, K.-H.; Ahn, S.-H., Hybrid manufacturing in micro/nano scale: A Review. *International Journal of Precision Engineering and Manufacturing-Green Technology* **2014,** *1* (1), 75-92.

[9] Abbas, N. M.; Solomon, D. G.; Bahari, M. F., A review on current research trends in electrical discharge machining (EDM). *International Journal of machine tools and Manufacture* **2007,** *47* (7), 1214-1228.

[10] Dubey, A. K.; Yadava, V., Laser beam machining—a review. *International Journal of Machine Tools and Manufacture* **2008,** *48* (6), 609-628.

[11] Kim, B. H.; Ryu, S. H.; Choi, D. K.; Chu, C. N., Micro electrochemical milling. *Journal of Micromechanics and Microengineering* **2004,** *15* (1), 124.

[12] Rajurkar, K.; Sundaram, M.; Malshe, A., Review of electrochemical and electrodischarge machining. *Procedia Cirp* **2013,** *6*, 13-26.

[13] Shin, H. S.; Park, M. S.; Kim, B. H.; Chu, C. N., Recent researches in micro electrical machining. *International Journal of Precision Engineering and Manufacturing* **2011,** *12* (2), 371-380.

[14] Martin, S.; Brown, P. S.; Bhushan, B., Fabrication techniques for bioinspired, mechanically-durable, superliquiphobic surfaces for water, oil, and surfactant repellency. *Advances in Colloid and Interface Science* **2017**.

[15] Tesler, A. B.; Kim, P.; Kolle, S.; Howell, C.; Ahanotu, O.; Aizenberg, J., Extremely durable biofouling-resistant metallic surfaces based on electrodeposited nanoporous tungstite films on steel. *Nature communications* **2015,** *6*, 8649.

[16] Park, B.; Hwang, W., A facile fabrication method for corrosion-resistant micro/nanostructures on stainless steel surfaces with tunable wettability. *Scripta Materialia* **2016,** *113*, 118-121.

[17] Bae, W. G.; Song, K. Y.; Rahmawan, Y.; Chu, C. N.; Kim, D.; Chung, D. K.; Suh, K. Y., One-step process for superhydrophobic metallic surfaces by wire electrical discharge machining. *ACS applied materials & interfaces* **2012,** *4* (7), 3685-3691.

[18] Bae, W.-G.; Kim, D.; Song, K. Y.; Jeong, H. E.; Chu, C. N., Engineering stainless steel surface via wire electrical discharge machining for controlling the wettability. *Surface and Coatings Technology* **2015,** *275*, 316-323.

[19] Chun, D.-M.; Ngo, C.-V.; Lee, K.-M., Fast fabrication of superhydrophobic metallic surface using nanosecond laser texturing and low-temperature annealing. *CIRP Annals-Manufacturing Technology* **2016,** *65* (1), 519-522.

[20] Ha, K. H.; Chu, C. N., Fabrication of an oil–water separation copper filter using laser beam machining. *Journal of Micromechanics and Microengineering* **2016,** *26* (4), 045008.

[21] Kietzig, A.-M.; Hatzikiriakos, S. G.; Englezos, P., Patterned superhydrophobic metallic surfaces. *Langmuir* **2009,** *25* (8), 4821-4827.

[22] Kwon, M. H.; Jee, W. Y.; Chu, C. N., Fabrication of hydrophobic surfaces using copper electrodeposition and oxidation. *International Journal of Precision Engineering and Manufacturing* **2015,** *16* (5), 877-882.

[23] Kwon, M. H.; Shin, H. S.; Chu, C. N., Fabrication of a super-hydrophobic surface on metal using laser ablation and electrodeposition. *Applied Surface Science* **2014,** *288*, 222-228.

[24] Chang, F.-M.; Cheng, S.-L.; Hong, S.-J.; Sheng, Y.-J.; Tsao, H.-K., Superhydrophilicity to superhydrophobicity transition of CuO nanowire films. *Applied Physics Letters* **2010,** *96* (11), 114101.

[25] Geng, W.; Hu, A.; Li, M., Super-hydrophilicity to super-hydrophobicity transition of a surface with Ni micro–nano cones array. *Applied Surface Science* **2012,** *263*, 821-824.

[26] Kim, D.; Kim, J. G.; Chu, C. N., Aging effect on the wettability of stainless steel. *Materials Letters* **2016,** *170*, 18-20.

[27] Liu, P.; Cao, L.; Zhao, W.; Xia, Y.; Huang, W.; Li, Z., Insights into the superhydrophobicity of metallic surfaces prepared by electrodeposition involving spontaneous adsorption of airborne hydrocarbons. *Applied Surface Science* **2015,** *324*, 576-583.

[28] Long, J.; Zhong, M.; Zhang, H.; Fan, P., Superhydrophilicity to superhydrophobicity transition of picosecond laser microstructured aluminum in ambient air. *Journal of colloid and interface science* **2015,** *441*, 1-9.

[29] Ta, D. V.; Dunn, A.; Wasley, T. J.; Kay, R. W.; Stringer, J.; Smith, P. J.; Connaughton, C.; Shephard, J. D., Nanosecond laser textured superhydrophobic metallic surfaces and their chemical sensing applications. *Applied Surface Science* **2015,** *357*, 248-254.

[30] Trdan, U.; Hočevar, M.; Gregorčič, P., Transition from superhydrophilic to superhydrophobic state of laser textured stainless steel surface and its effect on corrosion resistance. *Corrosion Science* **2017**.

[31] Zhang, Y.; Zou, G.; Liu, L.; Zhao, Y.; Liang, Q.; Wu, A.; Zhou, Y. N., Time-dependent wettability of nano-patterned surfaces fabricated by femtosecond laser with high efficiency. *Applied Surface Science* **2016,** *389*, 554-559.

[32] Ngo, C.-V.; Chun, D.-M., Fast wettability transition from hydrophilic to superhydrophobic laser-textured stainless steel surfaces under low-temperature annealing. *Applied Surface Science* **2017,** *409*, 232-240.

[33] Marchand, A.; Weijs, J. H.; Snoeijer, J. H.; Andreotti, B., Why is surface tension a force parallel to the interface? *American Journal of Physics* **2011,** *79* (10), 999-1008.

[34] Quéré, D., Wetting and roughness. *Annu. Rev. Mater. Res.* **2008,** *38*, 71-99.

[35] Shuttleworth, R.; Bailey, G., The spreading of a liquid over a rough solid. *Discussions of the Faraday Society* **1948,** *3*, 16-22.

[36] Young, T., An essay on the cohesion of fluids. *Philosophical Transactions of the Royal Society of London* **1805,** *95*, 65-87.

[37] Wenzel, R. N., Resistance of solid surfaces to wetting by water. *Industrial & Engineering Chemistry* **1936,** *28* (8), 988-994.

[38] Cassie, A.; Baxter, S., Wettability of porous surfaces. *Transactions of the Faraday society* **1944,** *40*, 546-551.

[39] Banerjee, S., Simple derivation of Young, Wenzel and Cassie-Baxter equations and its interpretations. *arXiv preprint arXiv:0808.1460* **2008**.

[40] Erb, R. A., Wettability of metals under continuous condensing conditions. *The Journal of Physical Chemistry* **1965,** *69* (4), 1306-1309.

[41] Mantel, M.; Wightman, J., Influence of the surface chemistry on the wettability of stainless steel. *Surface and Interface analysis* **1994,** *21* (9), 595-605.

[42] Trevoy, D. J.; Johnson Jr, H., The water wettability of metal surfaces. *The Journal of Physical Chemistry* **1958,** *62* (7), 833-837.

[43] Kalpakjian, S., *Manufacturing processes for engineering materials*. Pearson Education India: 1984.

[44] Adams, R., A review of the stainless steel surface. *Journal of Vacuum Science & Technology A: Vacuum, Surfaces, and Films* **1983,** *1* (1), 12-18.

[45] Takeda, S.; Fukawa, M., Role of surface OH groups in surface chemical

properties of metal oxide films. *Materials Science and Engineering: B* **2005,** *119* (3), 265-267.

[46] Takeda, S.; Fukawa, M.; Hayashi, Y.; Matsumoto, K., Surface OH group governing adsorption properties of metal oxide films. *Thin Solid Films* **1999,** *339* (1), 220-224.

[47] Tian, Y.; Su, B.; Jiang, L., Interfacial Material System Exhibiting Superwettability. *Advanced Materials* **2014,** *26* (40), 6872-6897.

[48] Verho, T.; Bower, C.; Andrew, P.; Franssila, S.; Ikkala, O.; Ras, R. H., Mechanically durable superhydrophobic surfaces. *Advanced Materials* **2011,** *23* (5), 673-678.

[49] Callister, W. D.; Rethwisch, D. G., *Fundamentals of materials science and engineering: an integrated approach*. John Wiley & Sons: 2012.

[50] Butler, I. B.; Schoonen, M. A.; Rickard, D. T., Removal of dissolved oxygen from water: a comparison of four common techniques. *Talanta* **1994,** *41* (2), 211-215.

[51] Hofmann, S., *Auger-and X-ray photoelectron spectroscopy in materials science: a user-oriented guide*. Springer Science & Business Media: 2012; Vol. 49.

[52] Watts, J. F.; Wolstenholme, J., An introduction to surface analysis by XPS and AES. **2003**.

[53] Jung, R.-H.; Tsuchiya, H.; Fujimoto, S., XPS characterization of passive films formed on Type 304 stainless steel in humid atmosphere. *Corrosion Science* **2012,** *58*, 62-68.

[54] Wagner, C. D., *Handbook of X-ray photoelectron spectroscopy*. Perkin-Elmer: 1979.

[55] Biesinger, M. C.; Payne, B. P.; Grosvenor, A. P.; Lau, L. W.; Gerson, A. R.; Smart, R. S. C., Resolving surface chemical states in XPS analysis of first row transition metals, oxides and hydroxides: Cr, Mn, Fe, Co and Ni. *Applied Surface Science* **2011,** *257* (7), 2717-2730.

[56] Masseria, V., *Metals Handbook: Heat Treating*. American Society for Metals: 1981.

[57] Hakiki, N.; Montemor, M.; Ferreira, M.; da Cunha Belo, M., Semiconducting properties of thermally grown oxide films on AISI 304 stainless steel. *Corrosion science* **2000,** *42* (4), 687-702.

[58] Cornell, R. M.; Schwertmann, U., *The iron oxides: structure, properties, reactions, occurrences and uses*. John Wiley & Sons: 2003.

[59] Demidov, A.; Markelov, I., Thermodynamics of formation of iron oxides and their hydrogen reduction. *Russian Journal of Applied Chemistry* **2010,** *83* (2), 232-236.

[60] Mittal, A.; Albertsson, G. J.; Gupta, G. S.; Seetharaman, S.; Subramanian, S., Some Thermodynamic Aspects of the Oxides of Chromium. *Metallurgical and Materials Transactions B* **2014,** *45* (2), 338-344.

[61] Padilha, A. F.; Plaut, R. L.; Rios, P. R., Annealing of cold-worked austenitic stainless steels. *ISIJ international* **2003,** *43* (2), 135-143.

[62] Tawfik, H.; Hung, Y.; Mahajan, D., Metal bipolar plates for PEM fuel cell—a review. *Journal of Power Sources* **2007,** *163* (2), 755-767.

[63] Peng, L.; Yi, P.; Lai, X., Design and manufacturing of stainless steel bipolar plates for proton exchange membrane fuel cells. *international journal of hydrogen energy* **2014,** *39* (36), 21127-21153.

[64] Perloff, D. S., Four-point sheet resistance correction factors for thin rectangular samples. *Solid-State Electronics* **1977,** *20* (8), 681-687.

[65] Chung, C.-Y.; Chen, S.-K.; Chiu, P.-J.; Chang, M.-H.; Hung, T.-T.; Ko, T.-H., Carbon film-coated 304 stainless steel as PEMFC bipolar plate. *Journal of Power Sources* **2008,** *176* (1), 276-281.

[66] Lee, S. W.; Shin, H. S.; Chu, C. N., Fabrication of micro-pin array with high aspect ratio on stainless steel using nanosecond laser beam machining. *Applied Surface Science* **2013,** *264*, 653-663.

[67] Shin, H.; Park, M.; Chu, C., Electrochemical etching using laser masking for multilayered structures on stainless steel. *CIRP Annals-Manufacturing Technology* **2010,** *59* (1), 585-588.

[68] Neergat, M.; Weisbrod, K., Electrodissolution of 304 stainless steel in

neutral electrolytes for surface decontamination applications. *Corrosion Science* **2011,** *53* (12), 3983-3990.

[69] Park, J. W.; Song, K. Y.; Chu, C. N., Fabrication of micro-lenticular patterns using WEDM-grooving and electrolytic polishing. *Journal of Micromechanics and Microengineering* **2013,** *23* (12), 125034.

[70] Park, J. W.; Kim, H.; Kim, J. G.; Chu, C. N., Fabrication of various shaped tungsten micro pin arrays using micro carving technology. *Precision Engineering* **2017,** *47*, 389-396.

[71] Seemann, R.; Brinkmann, M.; Kramer, E. J.; Lange, F. F.; Lipowsky, R., Wetting morphologies at microstructured surfaces. *Proceedings of the National Academy of Sciences of the United States of America* **2005,** *102* (6), 1848-1852.

국문 초록

철, 알루미늄, 구리 합금 등 엔지니어링 금속 표면의 젖음성 조절 기술은 자동차, 건설, 해양, 군사, 항공, 우주 등 다양한 분야에 적용되는 금속 재료의 기능성을 향상시킬 수 있는 전도유망한 기술이다. 연구실 규모에서 수행된 젖음성 조절 기술에 대한 다양한 연구 결과가 발표되고 있지만, 기술 상용화에 수반되는 여러 가지 문제점으로 인해 관련 기술이 실제 현장에 적용된 사례는 오늘날까지 찾기가 어렵다. 대표적인 문제로 엔지니어링 금속 표면에서 관측되는 에이징 효과를 들 수 있는데, 에이징 효과는 젖음성 조절을 위한 표면 가공 후 표면의 젖음성이 친수성에서 소수성으로 바뀌는 현상을 일컫는다. 에이징 효과로 인해 발생되는 문제로 인해, 다양한 노력에도 불구하고 초소수성과 초친수성 금속 표면을 제작하는데 있어 여전히 어려움이 있는 실정이다.

이 논문은 스테인리스강 표면 젖음성에 미치는 에이징 및 열처리의 영향에 대한 연구 결과를 제시한다. 거칠기가 최소화된 평평한 스테인리스강 304 시편 표면에서 에이징 효과의 존재를 실증하고 기저에 산소의 영향이 있음을 설명한다. 산소의 영향을 조절하기 위한 방안으로

금속 재료의 열처리를 통해 젖음성 조절이 가능함을 밝히고, 열처리 효과가 에이징 효과에 수반되는 문제점들을 해결할 수 있음을 제시한다. 최종적으로, 에이징과 열처리가 고려된 초소수성 및 초친수성 스테인리스강 표면 제작을 시연하여 논문의 연구 결과가 젖음성 조절 기술 상용화에 있어 장애물이 되고 있는 에이징 효과에 따른 문제점들을 해결할 수 있음을 실증한다.

주요어: 금속, 스테인리스강, 표면, 젖음성, 열처리

학 번: 2014-30336